

**Part I**

**The Academia – Market Bouncing of Peptide Drugs –  
Challenges and Strategies in Translational Research  
with Peptide Drugs**

COPYRIGHTED MATERIAL



# 1

## Peptides as Leads for Drug Discovery

*Paul J. Edwards and Steven R. LaPlante*

### 1.1 Introduction

Peptides have long been used as a source of active material for drug discovery but their use as marketed medicaments is often limited to intravenous administration. The received opinion for peptide drugs delivered via the oral route is that this is a highly challenging endeavor due to the peptides propensity for proteolytic degradation, high clearance, and resulting problems with its delivery, such as low oral bioavailability; all arising from the inclusion of a number of peptide bonds. Scientists have, therefore, sought peptide mimics (peptidomimetics) [1] where degradation of the peptide bonds is hindered (through, for example, N-methylation of the amide nitrogen) and de-peptidization through morphing of the amide (peptide) bonds into peptoids, for example, or through making the molecule more like a small molecule than a peptide. The peptidomimetic would have similar secondary structure as well as other structural features analogous to that of the original peptide, which allows it to displace the original peptide, or protein, from receptors or enzymes [2]. It is in the context of peptidomimics that this work will focus, on peptide-based discovery that has led to advanced (pre-)clinical candidates which are delivered by the oral route of administration.

Fortunately, advances in technologies such as phage-display screening, have enabled the high-throughput discovery of peptides that can inhibit a desired biological reaction for drug discovery purposes [3]. It is now also possible to enable the rapid optimization of peptide mimics to satisfy the many hurdles of drug development. This review intends to expose the fascinating properties and handles that peptides offer and how, through “sensemaking” – that is, the process of gathering and interpreting a body of information relevant to a problem [4] – leading to knowledge building within the project, coupled to synthetic and analytical strategies, successful processes may be adopted that can deliver peptide mimetic (pre-) clinical candidates. We will emphasize our experience from in-house programs where peptide leads were successfully advanced to pre-clinical and clinical candidates (see Figure 1.1). Critical lessons, novel strategies, and examples will be explored at various stages of this process, ranging from the discovery of peptide

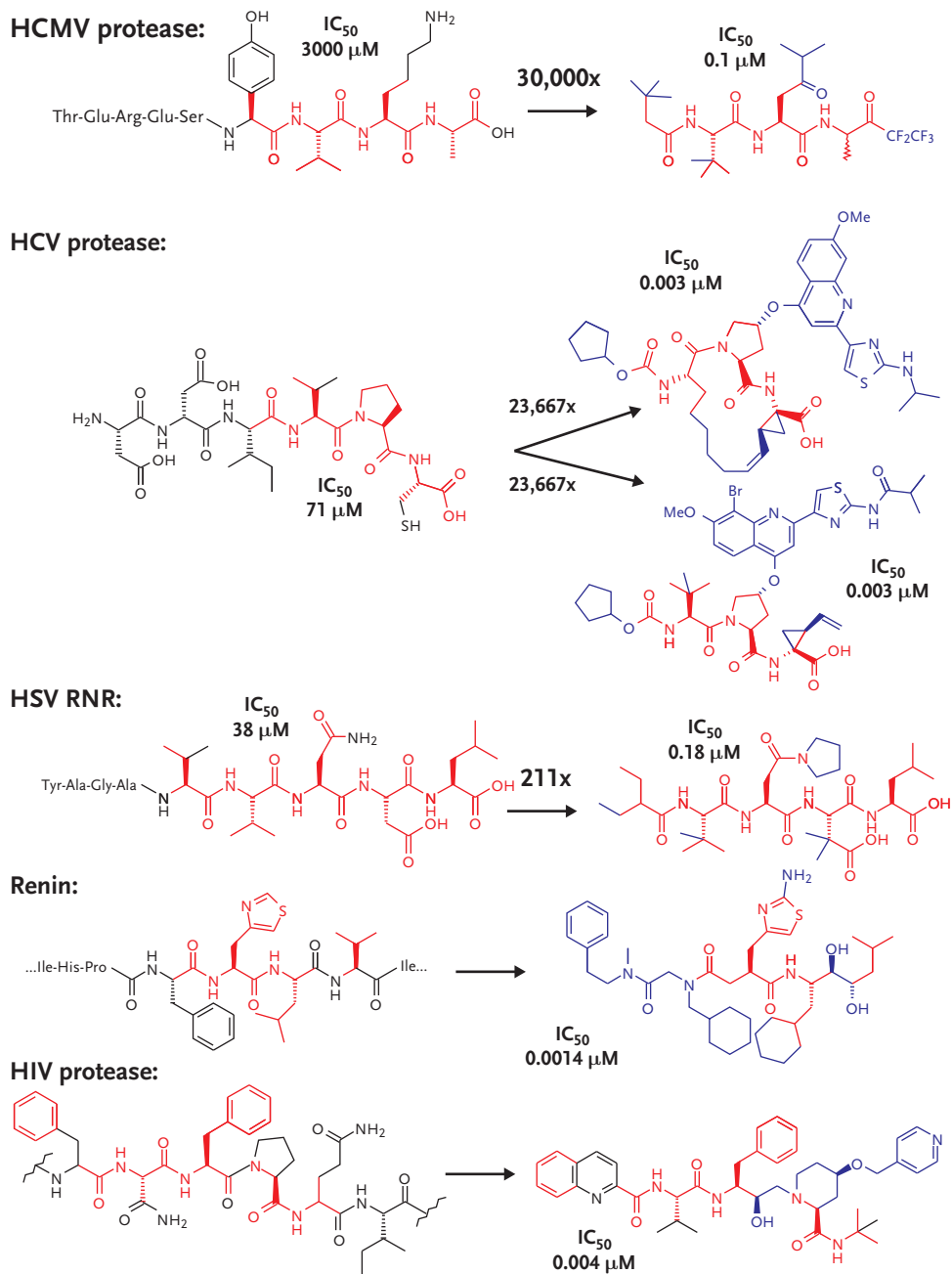


**Figure 1.1** Structures of peptide starting points (leads) and their advanced peptide mimics (drugs). The conserved bonds/atoms in both the lead and drug are colored red, whereas the blue and black represent new and modified or deleted sections, respectively.

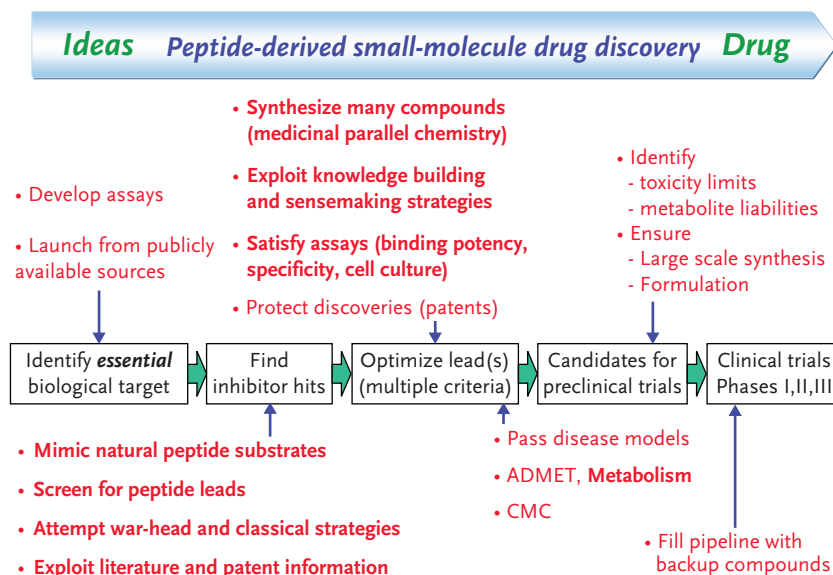
leads to those that have entered clinical trials. Particularly, we propose that our strategy and work flow (see Schemes 1.1 and 1.2) can represent an expeditious way to render peptides to drugs. This review will be based on exposing major findings/lessons that have commonality among systems and that can advance drug discovery rapidly, if used appropriately. Central for this purpose, it is demonstrated in Figure 1.1 that there can be a significant degree of similarity between the original peptide hit and the advanced analog. Figure 1.1 shows that one can conserve major segments and structural features of relatively weak lead peptides that are required for achieving potency in drugs (colored as red in Figure 1.1). Also critical are truncations and alterations (colored black) and the addition of new features (colored in blue). In summary, we believe that if one can exploit the latent structural functionality on the peptide starting points effectively, then delivery of orally bioavailable drugs derived from a peptide lead becomes possible.

## 1.2

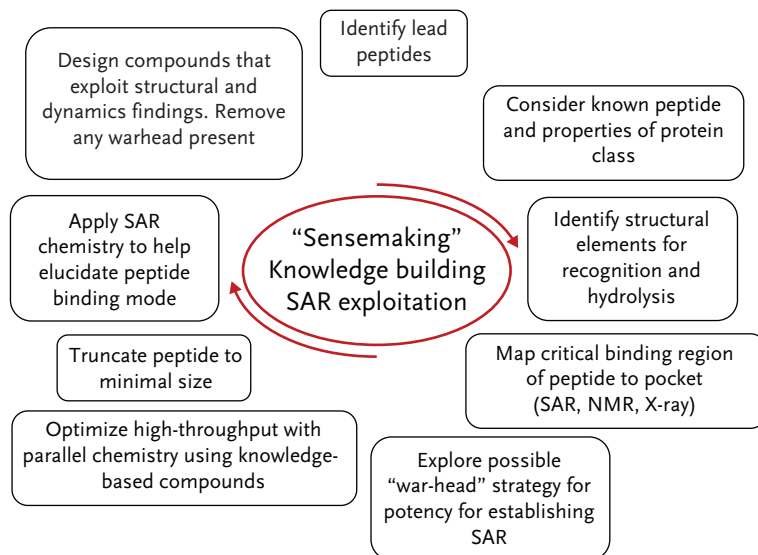
### Overview of Process for Transforming Peptides to Peptidomimetics

The pharmaceutical industry has developed complex and fascinating processes for discovering and optimizing leads that become drugs. Scheme 1.1 depicts an overview of how one might progress a peptide to peptidomimetic drug project, indicating the various stages (bold text) that will be exemplified in the projects that follow. Of central importance is the “sensemaking” phase (Scheme 1.2), supported by knowledge building, including mapping of the critical binding parts of the peptide with model creation and peptide truncation, and matching of the free state of the peptide to the bioactive conformation through, for example, rigidification, and de-peptidization.

This chapter will consider a number of case studies against different targets where, after hit identification, the minimal peptide fragments were elucidated and then subjected to conformational rigidification. It is well understood that the binding of a ligand to a macromolecule involves numerous recognition events that are strongly influenced by forces such as van der Waal contacts, electrostatic interactions, solvation effects, and also by ligand to macromolecule shape complementarity. Less well appreciated, but no less important and as critical to these recognition events, are the necessary structural and flexibility adaptations of the ligand and receptor to attain the bioactive complex. Therefore, when considering utilizing a peptide hit as a starting point for drug discovery, the tactics utilized should move beyond the classical “lock-and-key” model to a more holistic approach that incorporates the effects of dynamics and conformational changes. In doing so, rational drug design efforts could be accelerated from the knowledge of these adaptive processes. However, to date, few reports of the application of dynamics and conformational changes have appeared in the literature. In part this is due to the paucity of experimental methods that can provide the type of atomic-level information required. Thus, their importance and impact in drug design have not yet been fully realized.



**Scheme 1.1** An overview of the peptide-derived, small-molecule drug discovery. Highlighted in bold text are discovery periods where “sensemaking” and knowledge building cycles can be employed during peptide optimization.



**Scheme 1.2** An overview of the drug discovery periods that impact and fuel the “sensemaking,” knowledge building, and SAR exploitation cycles.

The process we propose may be summarized (Scheme 1.2) as follows:

- Identify lead peptides.
- Understand properties of the protein.
- Map critical binding elements of substrate peptide.
- Understand (by X-ray/NMR) protein–ligand interactions.
- Increase potency, for example, by using a warhead if necessary, to provide meaningful structure–activity relationships (SAR).
- Truncation to minimally active peptide (allowing for initial losses in potency as needed).
- Elucidate free versus bound conformations and ensure SAR designs produce compounds with free conformations matching the bioactive one.
- In parallel, de-peptidize molecule (e.g., by including bulky side-chains or altering the backbone) and remove any warhead present.

This process will be exemplified through the following examples.

### 1.3

#### HCMV Protease

##### 1.3.1

#### **HCMV Protease: Identification and Characterization of Antiviral Inhibitors Targeting the Serine Protease Domain of the Human Cytomegalovirus (HCMV Protease)**

Human Cytomegalovirus (HCMV) is a pathogen and member of the herpesvirus family that is highly prevalent in the human population [5]. This virus poses a significant risk to immunocompromized individuals, organ transplant recipients and neonates who acquire the infection congenitally [6, 7]. HCMV encodes a unique protease involved in capsid assembly and this protease enzyme is responsible for processing the assembly protein; the latter protein's function is analogous to that of the “scaffolding” protein of bacteriophages [8] and its activity is essential to the production of infectious virions [9–12].

The full-length HCMV protease precursor contains 708 amino acids encoded by the UL80 gene. It was discovered that the enzyme can process its own C-terminus and that the protease can also undergo self-processing at the release site near its amino terminus. This cleavage liberates the 256 amino acid catalytic domain, or HCMV protease. Although this enzyme belongs to the serine protease family, differences between familial members exist, as evidenced through X-ray crystallographic analyses [13–16]. These analyses have shown that it possesses a unique protein fold and an unusual catalytic triad (a histidine replacing the more common aspartate). Additionally its activity arises exclusively from its dimer form [17, 18]. Spectroscopic studies [19] have demonstrated that the binding of substrate-based competitive inhibitors results in a conformational change in the enzyme and that catalysis by HCMV protease is performed through an “induced fit” model [20, 21]. Faced with a need to develop a potent HCMV protease inhibitor, the following research process was undertaken.

## 1.3.2

**Mapping Essential Elements of the Substrate Peptides and Determining Structures of Ligands Bound to HCMV**

As substrate hydrolysis by HCMV protease was essential for viral capsid assembly, the first task was to decipher the minimal structural elements of the substrates that were required for recognition and hydrolysis. Enzymological studies revealed that peptides which corresponded to 17 amino acids of the release- and maturation-sites (R-site and M-site peptides) were sufficient to induce hydrolysis by HCMV protease (Figure 1.2) [21]. Substitutions of amino acids of the P' residues (using standard nomenclature [22]) had less of an effect on oligopeptide substrate hydrolysis rates than those of P-side residues [23].

Differential line-broadening (DLB) NMR was then valuable for understanding which residues were playing a direct role in the binding of the substrate and product recognition by the enzyme [21]. The DLB method [24] provides atomic-resolution data and was used as a tool within the project to assess ligand binding. As Figure 1.3a shows, using the N-terminal product peptide (R-product) of the release-site, albeit a weak inhibitor ( $IC_{50} \sim 3000 \mu\text{M}$ ), it nevertheless bound to the protease, as indicated by the selective resonance perturbations observed when the hydrogen resonances of the peptide were compared in the absence versus presence of HCMV protease (Figure 1.3a). The changes in the peak shape and intensity resulted from fast-exchange averaging between the free and bound states (Figure 1.3b). The broadened resonance of the methyl group of Ala 1 (comparing

	...P9 P8 P7 P6 P5 P4 P3 P2 P1  P1' P2' P3' P4' ...P8'	$\frac{k_{\text{cat}}}{K_M}$ ( $\text{M}^{-1}\text{s}^{-1}$ )
<b>R-site</b>	Thr-Glu-Arg-Glu-Ser-Tyr-Val-Lys-Ala - Ser-Val-Ser-Pro...	42
<b>R-mutant</b>	... Asn ...	282
<b>M-site</b>	Arg-Ala-Gln-Ala-Gly-Val-Val-Asn-Ala - Ser-Cys-Arg-Leu...	657
<b>M-mutant</b>	... Lys ...	54
		<b><math>IC_{50}</math></b> ( $\mu\text{M}$ )
<b>R-product</b>	Thr-Glu-Arg-Glu-Ser-Tyr-Val-Lys-Ala	$\sim 3000$
<b>M-product</b>	Arg-Ala-Gln-Ala-Gly-Val-Val-Asn-Ala	$> 1000$
<b>1</b>	Gly-Val-Val-Asn-Ala- $\text{CF}_3$	1.8

**Figure 1.2** Amino acid sequences of peptides/inhibitors with enzymological ( $k_{\text{cat}}/K_M$ ) and inhibitory activity ( $IC_{50}$ ) data [21]. The nomenclature used to denote amino acid positions is given above (i.e., P9 to P4') [22]. The peptides labeled as R-site, R-mutant, M-site, and M-mutant are 17 amino acids in length, but only the sequence to P4' is provided for space-saving. The full sequence can be found elsewhere [21]. Reproduced with kind permission from Springer Science + Business Media: *Top. Curr. Chem.*, Exploiting Ligand and Receptor Adaptability in Rational Drug Design Using Dynamics and Structure-Based Strategies, 272, 2007, 264, Steven R. LaPlante, Figure 2.

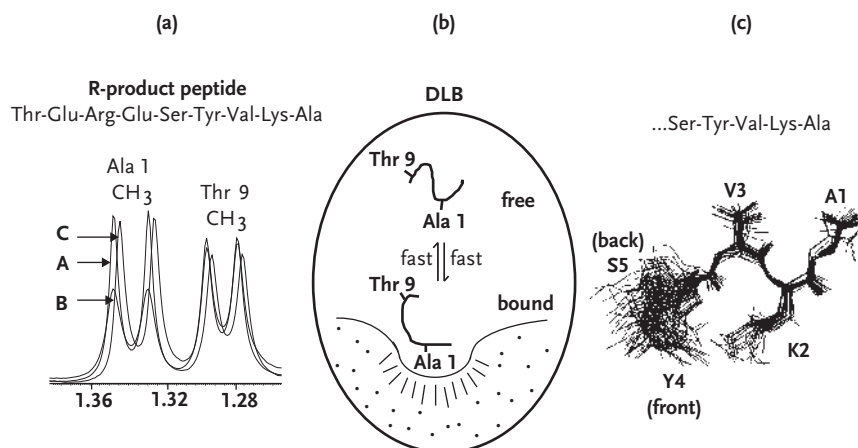


**Figure 1.3** DLB mapping that distinguished between residues that were solvent exposed versus those that directly contact the receptor. Shown is the methyl region of the  $^1\text{H}$  NMR spectrum of R-product showing the P1 and P9  $\text{CH}_3$  side-chain doublets [21]. (a) A, free R-product; B, R-product after the addition of HCMV protease at a ratio of 7 : 1; and C, R-product after the addition of HCMV protease and the more potent inhibitor **6** for displacement purposes at a 7 : 1 : 2 ratio. For the sake of clarity, the P1 methyl signals have been skewed slightly. (b) Demonstrates that the DLB method requires fast-exchange binding (averaging) between the free and bound states (on the NMR timescale). (c) The 3D structure of the P5–P1 sequence of R-product when bound to HCMV protease. The 32 overlapped structures determined were derived using transferred NOESY restraints and simulated annealing calculations. Reproduced with kind permission from Springer Science + Business Media: *Top. Curr. Chem.*, Exploiting Ligand and Receptor Adaptability in Rational Drug Design Using Dynamics and Structure-Based Strategies, 272, 2007, 265, Steven R. LaPlante, Figure 3.

“A” with “B” in Figure 1.3a) was due to this group becoming pocket exposed upon binding to HCMV (see the illustration in Figure 1.3b). In contrast, the  $^1\text{H}$  resonance of the methyl group of Thr 9 changed little, as expected for a group that was predominantly solvent exposed in the free and bound states. Using this method, the ensembles of DLB patterns were monitored for the R-product and M-product peptides, and it was discovered that the P4 to P1 residues directly contacted the protease whereas the P9 to P5 residues were solvent exposed [21].

This was also consistent with enzymology findings that peptides spanning the P4–P1' M-site core were capable of competitively inhibiting catalysis with binding affinity only fivefold less than that of the P4–P4' substrate [25]. Overall, the ensemble of data indicated that the structural elements of the substrate which were N-terminal to the scissile bond were clearly crucial for complexation to the enzyme. Thus, the first step in the process of identifying the critical binding parts of the substrate peptides has been completed (i.e., P4–P1).

There was also enzymology effort applied to identifying the (peptide) source of the different processing rates observed between the R-site and M-site peptides (Figure 1.2). Enzymology studies followed that mutated the R-site and M-site peptide substrates (i.e., P5 and P4 residues were separately exchanged), as well as

through substitution of the P2 residue of the R-site peptide to that of the M-site (Lys to Asn, and called R-mutant in Figure 1.2). It was discovered that the P2 side-chain played a major role in the observed variation in cleavage rates, suggesting that this P2 side-chain influenced the catalytic triad reactivity and so was integral to modulating the catalytic machinery (i.e., shielding the catalytic triad from solvent effects). It was also envisioned that a better understanding of this phenomenon could be exploited for inhibitor potency improvements. Although the promise of this phenomenon was not sufficiently explored in our HCMV protease program, it was successfully exploited in our efforts at optimizing the P2 position in our HCV protease peptidomimetic program, as described later in this chapter.

### 1.3.3

#### Improving Peptide Activity to Allow SAR Studies

Serine proteases are a well-studied class of enzyme [26–28]. Despite significant differences in global protein architecture, they possess similar catalytic machinery (triad), which is thought to arise from convergent structural evolution at the enzyme level. The frequently considered “warhead” strategy was, therefore, employed to create substrate-based activated carbonyl inhibitors [29] to boost potency (i.e., compound **1** in Figure 1.2). The improvement in activity also allowed the generation of meaningful SAR. Warheads involved the synthesis of electrophilic ketones which replaced the C-terminus acid of the N-terminal cleavage products [30]. By allowing attack upon the active-site serine, covalent hemiketal adducts were formed that mimic the transition state of the tetrahedral intermediate formed during the catalytic reaction. In this way, a boost in potency was observed with compound **1** (HCMV protease  $IC_{50}$  1.8  $\mu$ M) [19, 30], compared to the corresponding M-product peptide containing a C-terminal carboxylate ( $IC_{50} > 1000 \mu$ M; Figure 1.2).

With this improved potency, meaningful SAR then became possible. N-terminal truncation of P5 gave an inhibitor with similar potency (e.g., compare compound **1** versus **2** in Figure 1.4), but losses in potency were observed upon further truncation of the P4 and P3 residues (e.g., compare compound **2** with **3** and **4** in Figure 1.4) [30]. Thus, the P4 to P1 peptidyl segment, as suggested by the NMR experiments described above, played a critical role in ligand binding to the active-site of HCMV protease. Further chemistry efforts focussed on optimizing each of the P1–P4 substituents in turn; once one position had been improved significantly, this moiety was incorporated into optimization of the next position along in the sequence. In this way, the best P2 group was as indicated in compound **2** ( $IC_{50}$  3  $\mu$ M) and the best P3 was found to be the *tert*-butyl group (compound **5**;  $IC_{50}$  1.1  $\mu$ M).

### 1.3.4

#### Elucidation of the Binding Mode of the Optimized Peptidyl Segment

Contemporaneous with medicinal chemistry efforts to determine which substituents controlled binding and activity, structural research efforts focussed on

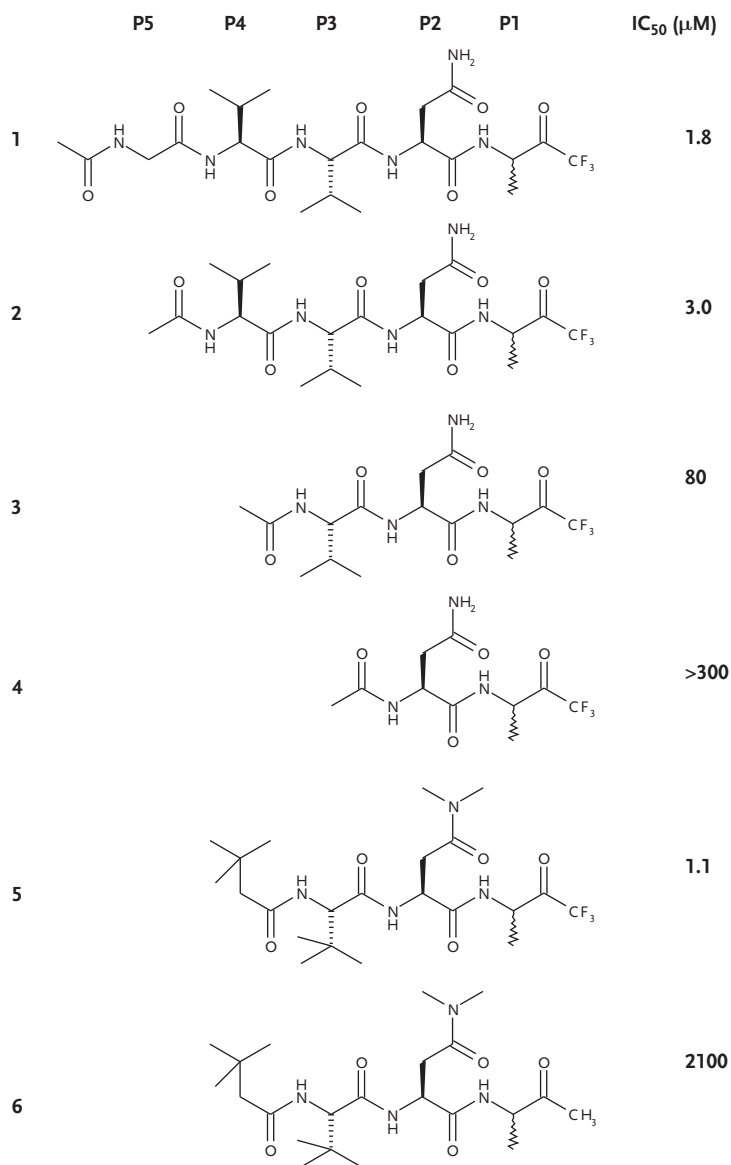


**Figure 1.4** Inhibitors 1–6 with inhibition constants. The amino-acid positions are designated on top as P5–P1.

determining the binding mode of these compounds when bound to HCMV protease. It did not prove possible to use the technique of transferred NOESY (nuclear Overhauser spectroscopy) to determine bound conformation, so ligands were designed that as closely as possible resembled the peptidyl portion of the inhibitors without providing the slow exchange phenomenon arising from inactivation of the

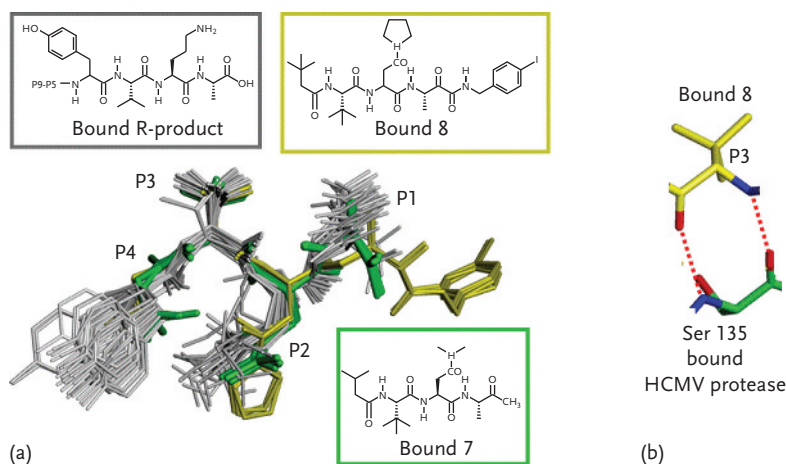


**Figure 1.5** (a) Overlap of NMR-derived bound conformations of compound **7** (colored green; 29 conformations), R-product peptide (gray; 32 structures), and the X-ray crystallographic conformations of bound compound **8** (yellow; 4 conformations). (b) Zoomed view of the P3–S3 interaction of compound **8** bound to HCMV protease. Reproduced with kind permission from Springer Science + Business Media: *Top. Curr. Chem.*, Exploiting Ligand and Receptor Adaptability in Rational Drug Design Using Dynamics and Structure-Based Strategies, 272, 2007, 269, Steven R. LaPlante, Figure 7.

enzyme caused by highly electrophilic warhead groups. Thus, methyl ketones **6** [31] and **7** (Figures 1.4 and 1.5, respectively) were designed as NMR-friendly structural probes that could not form covalent complexes when bound to the enzyme, and exhibited fast exchanging binding attributes. In contrast, fluoroketone **5** (Figure 1.4) formed a slow-exchange covalent complex, as determined by  $^{13}\text{C}$  NMR experiments [19].

Thus, replacing the C-terminal  $\text{CF}_3$  with a  $\text{CH}_3$  provided compounds unreactive toward attack by the active-site serine and so provided a useful structural probe of the bioactive conformation. Transferred NOESY data on compound **7** (*vide infra*, Figure 1.5a) and the derived distance restraints were applied to determine the family of bound structures shown in green in Figure 1.5a [31]. These studies indicated that they all bound in the extended conformation with a zigzagged backbone, with the P1 and P3 side-chains lying close to one another, and similarly for the P2 and P4 side-chains. The commonality of this structural feature for all three compounds suggested that this bioactive conformation played an important role for binding and activity. The dramatic losses in potency observed upon N-terminal truncation of P4 and P3 was consistent with this observation.

### 1.3.5

#### Ligand Adaptations upon Binding

There followed a stage in the project where compounds were designed that preferentially adopted the bioactive conformation in the free-state. Dramatic

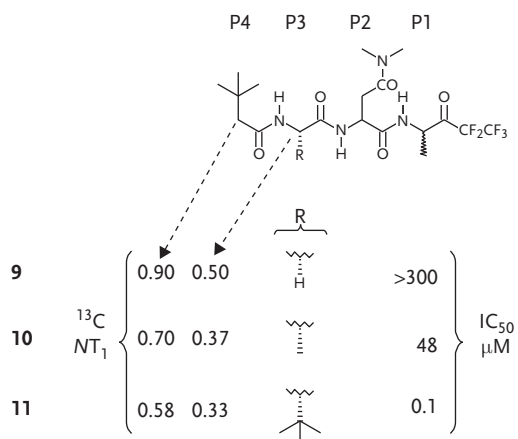


**Figure 1.6** Inhibitors 9–11 with inhibition constants.  $^{13}\text{C}$   $T_1$  relaxation data are given for the P3  $\text{C}\alpha$  carbon. For the methylene carbon which has two covalently attached hydrogens,  $NT_1$  values are provided, where  $N$  is the number of attached hydrogens, to help in interpreting the relative flexibility between different carbon types. Reproduced with kind permission from Springer Science + Business Media: *Top. Curr. Chem.*, Exploiting Ligand and Receptor Adaptability in Rational Drug Design Using Dynamics and Structure-Based Strategies, 272, 2007, 270, Steven R. LaPlante, Figure 8.

improvements in potency were attained (Figure 1.6) when a glycine at P3 (compound 9,  $\text{IC}_{50} > 300 \mu\text{M}$ ) was replaced with an alanine (compound 10,  $\text{IC}_{50} 48 \mu\text{M}$ ) or a *tert*-butyl group (compound 11,  $\text{IC}_{50} 0.1 \mu\text{M}$ ) [30]. These increases in potency could not be explained by direct contacts with the protease pocket alone. The more overwhelming source for the improvements in potency was a result of the incorporation of the bulkier side-chains which helped to rigidify the compounds to resemble the bioactive conformation.

The relative rigidity (or flexibility) of these compounds was monitored by the NMR technique  $^{13}\text{C}$  spin–lattice relaxation measurements ( $^{13}\text{C}$   $T_1$ ) [20]. Overall, shorter relaxation times are indicative of less flexibility. These experiments indicated that the conformational restriction induced by the bulkier P3 side-chain resulted in a minimization of the overall entropic cost of binding. The bulky group forced the critical P3 backbone into the bioactive, extended conformation in the free state which aided in the formation of two hydrogen bonds that were required upon complexation with HCMV protease (see Figure 1.5b) [20, 32].

In considering the ensemble of mounting information and given the highly related findings in our HSV RNR, HCV protease, and HIV protease programs, as described below, the principle of an easily synthesizable, Val or *tert*-butyl side-chain group, certainly proved to be a valuable medicinal chemistry tool, allowing significant improvements in inhibitor potency, where its incorporation is appropriate.

Later in the HCMV program, a peculiar observation was noted where a significant adaptation of the receptor was seen upon substrate or peptidomimetic

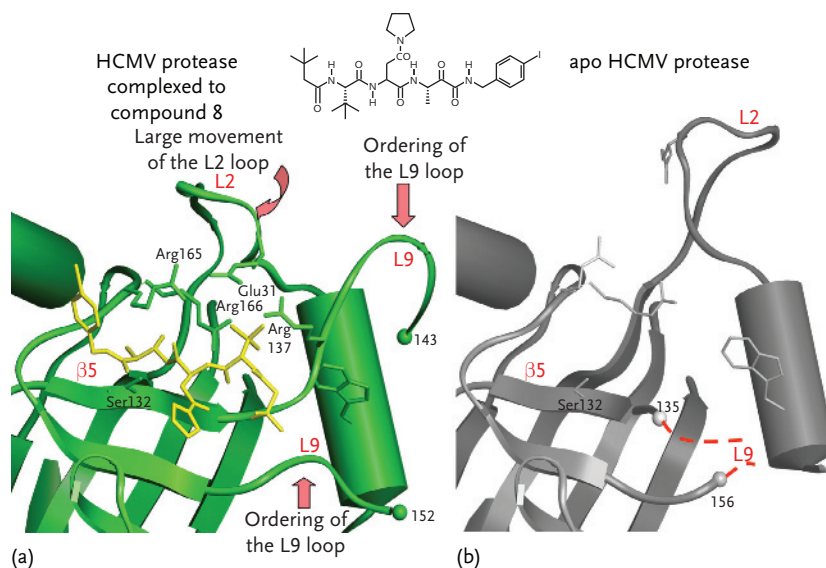


**Figure 1.7** Peptidyl ligand-induced conformational changes of HCMV protease. Views of the active site region of (a) the inhibited enzyme (in green) covalently bound with ketoamide **8** shown in yellow and (b) the apoenzyme (in gray). Spheres indicate the points at which there was no electron density further along the L9-loop. Reproduced with kind permission from Springer Science + Business Media: *Top. Curr. Chem.*, Exploiting Ligand and Receptor Adaptability in Rational Drug Design Using Dynamics and Structure-Based Strategies, 272, 2007, 273, Steven R. LaPlante, Figure 11.

binding, as supported by X-ray structure and fluorescence methods (Figure 1.7). In this respect, the process bears elements of protein conformer selection [33]; the peptide guiding the reorganization of the protein around it after association. At this stage of the project, the “sensemaking” indications were that a prerequisite rigidification of the pocket upon peptidyl ligand binding could represent a minimal ceiling in terms of the entropic cost of binding. Thus, this intrinsic feature may ultimately limit any further potency improvements.

In fact, many of our further efforts, and those of competing companies, failed to improve the potency of the peptidyl-activated carbonyl inhibitors. This failure was consistent with the concept of an energetic penalty for protein reorganization on ligand binding. Thus, in this case, many companies aborted efforts at discovering peptidomimetics targeted at this protease (virus). We believe that we went one step further by reasoning that a promising path would be to screen for inhibitors favoring the flexible apo receptor, as we found for beta-lactam inhibitors [5, 20].

### 1.3.6

#### Strategic Summary for HCMV Peptide Mimic Design Process

Inhibition of HCMV protease by the peptidyl compounds described above involved the binding of the peptidyl portion to morph the transition state to a catalytically

active or activated form of the enzyme. With HCMV protease, an induced-fit catalysis results in binding energy that is expended to compensate for the energy required to convert the enzyme to a thermodynamically less favorable state.

This then explains our strategy of identifying the first lead inhibitor, whereby a C-terminal warhead was incorporated onto N-terminal product peptides. The warhead induced a reversible, covalent mode of binding that mimicked the transition state of substrate cleavage and was utilized to facilitate meaningful SAR studies. However, due to toxicity concerns of deleterious interactions between warheads and proteins, the removal of the warhead from inhibitors was sought, once a level of inhibitor potency had been obtained that allowed the generation of meaningful SAR within the program.

First, the core scaffold of the ligand involved in direct binding to the protease was discovered, followed by utilization of NMR methods to monitor the bioactive conformation of these inhibitors, including the dependence of potency on the free-state flexibility. More potent compounds exhibited similar free and bound (bioactive) conformations, resulting in a reduction in the entropic cost of binding.

Another important finding was that the active-site underwent conformational adaptations upon binding the peptidomimetic ligands and substrates, characterizing HCMV protease as an induced-fit enzyme. The resultant entropic cost required to induce the “activated” state meant there was an intrinsic cost involving the receptor due to changes upon binding. Consistent with this, we and others could not improve inhibitor potencies. In the end, potent ligands were successfully obtained, but the necessity for protein rearrangement precluded further progression of this series of compounds. Throughout this campaign, novel strategies were developed to monitor the bioactive conformation and changes in flexibility of the ligands and receptor. Fortunately, the general nature of these strategies was later applied with success to a highly related campaign that targeted the HCV protease.

## 1.4 HCV Protease

### 1.4.1 HCV Protease as an Antiviral Target

Up to 200 million people around the world are infected with the hepatitis C virus [34]. The majority of individuals with persistent HCV infection will develop chronic hepatitis C, a progressive liver disease that can lead to cirrhosis and hepatocellular carcinoma [35–38]. HCV is an enveloped RNA virus belonging to the Flaviviridae family and Hepacivirus genus. As is typical for this family, its positive-sense RNA genome (9.5 kb) encodes a single precursor polyprotein which undergoes proteolytic maturation by enzymes that include host signalases and the viral NS2/3 protease and NS3 protease. NS3 protease (also referred to as HCV protease) is responsible for cleaving four of its non-structural (NS) proteins.

## 1.4.2

**NS3 Serine Protease Possesses a Chymotrypsin-Like Fold**

The cleavage sequences have little homology, with the following exceptions: three of four sites have a serine at P1' and a cysteine at P1, and all four sites have an acidic amino acid at P6 (colored blue, Figure 1.8). Given this permissivity, we employed a peptide substrate having the sequence DDIVPC-SMSYTW [39] for *in vitro* enzymology studies/assays (colored orange, Figure 1.8).

## 1.4.3

**Discovery of the Peptide DDIVPC as an Inhibitor of NS3 Protease**

Initial efforts focussed on the approach of designing substrate-based activated carbonyl inhibitors which involved the synthesis of N-terminal cleavage products in which the acid of the C-terminus is replaced with an electrophilic ketone. Upon attack by the active-site serine, a stable covalent hemiketal adduct is formed that mimics the transition state of the tetrahedral intermediate formed during the

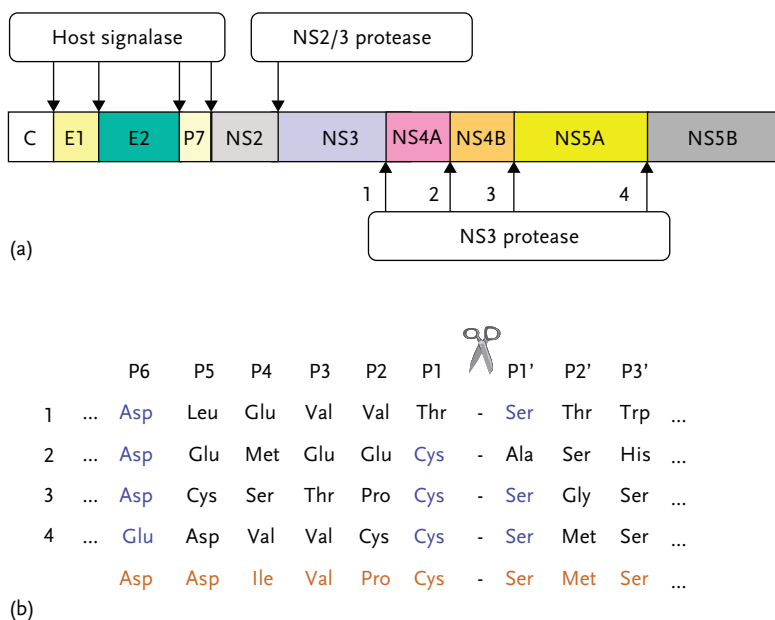
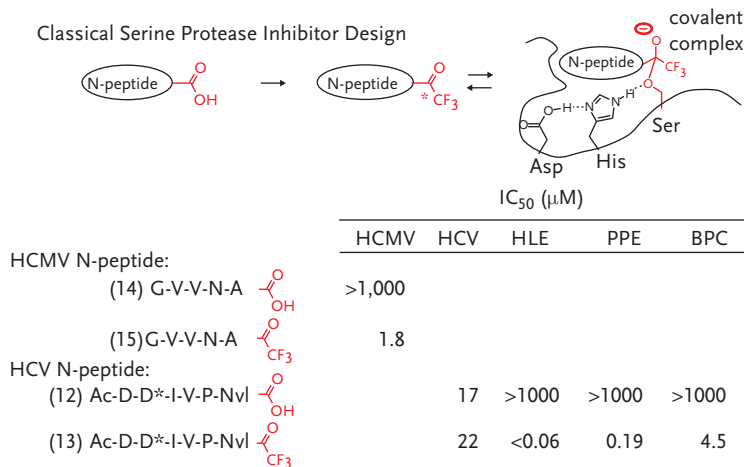


**Figure 1.8** (a) An illustration of the polyprotein encoded by the HCV genome, together with the processing cleavage sites. (b) Sites and sequences cleaved by NS3 protease. The amino-acid positions are designated on top as P6–P3'. The numbers to the left correspond to the numbered sites in (a). Also shown is a model sequence used for enzymology studies and assays (colored orange). Consensus residues are colored blue. Reproduced with kind permission from Bentham Science Publishers Ltd.: *Curr. Med. Chem. – Anti-Infective Agents, Dynamics and Structure-based Design of Drugs Targeting the Critical Serine Protease of the Hepatitis C Virus – From a Peptidic Substrate to BILN 2061*, 4, 2005, 113, Steven R. LaPlante and Montse Llinàs -Brunet, Figure 2(A).

catalytic reaction [26–28]. Concurrent to this work, we sought to determine the bioactive conformation of bound peptidyl ligands through transferred NOESY NMR methods. Since slow binding ligands, such as activated carbonyl inhibitors, are not suitable for such studies [31], our efforts were directed to the synthesis of N-terminal cleavage peptides having an acid C-terminus. Surprisingly, the activity of the N-terminal product peptide DDIVPC of NS3 protease was more active than expected ( $IC_{50}$  71  $\mu$ M), thus this became the initial inhibitor lead for further SAR efforts [40]. The next efforts were to replace the reactive cysteine at P1 of DDIVPC with a chemically more stable residue and norvaline was found to be a stable replacement with only a fivefold loss in potency [41]. This loss was then recovered by the replacement of P5 by D-Asp and the addition of a P6 acetyl, resulting in compound **12** having an  $IC_{50}$  value of 17  $\mu$ M. Efforts were then refocussed on replacing the C-terminal acid with an activated-carbonyl warhead to provide an expected boost in activity. However, the C-terminal acid and trifluoromethylketone analogs exhibited comparable activity (compounds **12** and **13** in Figure 1.9) [41].

Unlike the case of HCMV protease, where only compounds with an activated carbonyl were active enough to be considered as a lead for optimization (compound **15** is much more active than **14**, as shown in Figure 1.9) [20, 30], both product

### Unique product inhibition by C-terminal COOH peptides



### C-terminal carboxylate provides multiple advantages !

**Figure 1.9** Inhibitors of HCMV and HCV are shown with inhibition constants determined using various enzymes. The amino acid positions are designated on top as P6–P1. The inhibition constants involving HCV were determined using the NS3 protease domain and an NS4A peptide [41]. The other binding constants were determined as described elsewhere [30, 40]. The abbreviations for the proteases are defined as follows: HCV, hepatitis C virus; HLE, human leukocyte elastase; PPE, porcine pancreatic elastase; BPC, bovine pancreatic chymotrypsin; HCMV, human cytomegalovirus protease. Selectivity targets were chosen because they represented closely-related chymotrypsin-like serine proteases, when compared to HCV protease.

peptide and activated carbonyl inhibitors of NS3 protease (compounds **12** and **13**) [40–42] had similar potency and were viable starting points as leads. However, the C-terminal acid (compound **12**) had superior attributes to the trifluoromethylketone N-peptide (compound **13**). For example, compound **12** had a superior selectivity profile, as compared to other serine proteases shown in Figure 1.9. Figure 1.9 shows that compound **13** inhibits human leukocyte elastase (HLE) with an  $IC_{50} < 0.06 \mu\text{M}$ . In contrast, the C-terminal carboxylate inhibitor (compound **12**) provides high specificity for NS3 protease with an  $IC_{50} 17 \mu\text{M}$  versus  $IC_{50} > 1000 \mu\text{M}$  for other typical serine proteases (e.g., human leukocyte elastase, porcine pancreatic elastase, and bovine pancreatic chymotrypsin) [41]. Warheads would be expected to show reduced selectivity toward other proteins and, hence, would be expected to contribute to greater inhibitor toxicity than the carboxylic acid group. The C-terminal carboxyl derivatives also exhibit other favorable qualities, such as chemical stability and aqueous solubility at neutral pH. For all of the above reasons, the carboxylic acid group was preferred over a warhead for inclusion in inhibitor design for this project.

#### 1.4.4

##### **“Sensemaking” and Knowledge Building: Mapping of the Critical Binding Residues of the Peptide and Creation of an Inhibitor-Protease Model**

In trying to improve inhibitor potency by modifying the side-chains and reducing the peptidic nature of our early peptides, medicinal chemists undertook a synthetic study in which single amino acid changes (natural and unnatural) were incorporated into hexapeptides, and the effect on potency was monitored. This exercise led to the finding that a benzylmethoxy proline at P2 (compound **16**, Figure 1.10) resulted in a 21-fold improvement in potency (compound **17** versus **18**, Figure 1.11) [43, 44].

To help guide medicinal chemistry efforts, a ligand-focussed NMR strategy was undertaken to determine which sites of the peptides contacted the protease and which were solvent exposed in the bound state [43, 45]. The differential line-broadening (DLB) NMR experiment [24, 45] was used and, in general, ligand sites that contacted the protease could be identified by specific broadening of the corresponding NMR resonances upon addition of small amounts of protease. When applied to DDIVPC and longer sequences spanning P10–P1, it was found that only specific resonances of P4–P1 experienced broadening (Figure 1.10a and b). No broadening was observed for peptides corresponding to the P' sequences. This suggested that smaller compounds spanning only P4–P1 should retain a reasonable binding affinity [43].

#### 1.4.5

##### **Knowledge Building: Monitoring Ligand Flexibility in the Free-State and Changes Upon Binding – P3 Rigidity**

Next we sought to identify any differences that may exist for compound **16** between the free and bound states. Distance information from the bound state was monitored by the transferred NOESY experiment (Figure 1.10c), and the free state

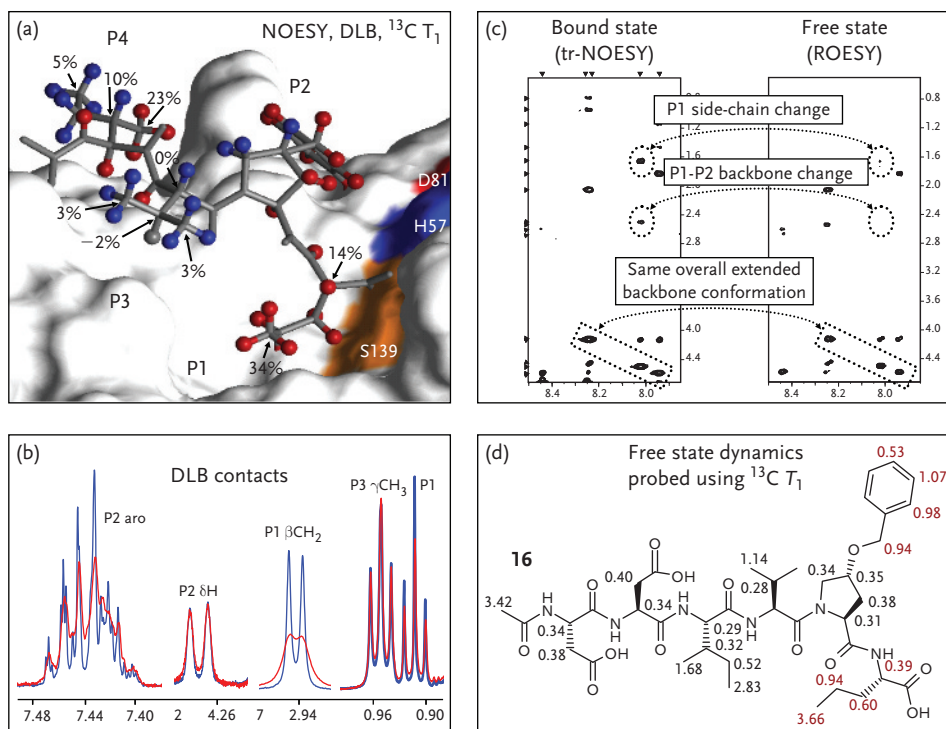


**Figure 1.10** “Sensemaking” using NMR-based knowledge building that probed both structure and dynamics information. (a) The first model of the complex between compound **16** and NS3 protease, with a summary of DLB perturbation mapping data, and transferred <sup>13</sup>C T<sub>1</sub> data. The complex was determined by docking the bound structure of compound **16** (experimentally determined by transferred NOESY NMR data) to an *apo* X-ray structure of NS3 protease. For the DLB mapping data, hydrogens of compound **16** are colored blue for resonances in which no broadening perturbations were observed upon binding protease, and hydrogens are colored red when significant resonance broadening was observed upon binding. P5 and P6 were determined to be relatively flexible in the bound state and are not shown above. A summary of the transferred <sup>13</sup>C T<sub>1</sub> data (placed next to each carbon) is also displayed as the percentage change in <sup>13</sup>C T<sub>1</sub> before and after the addition of NS3 protease. (b) DLB perturbation data. Selected <sup>1</sup>H NMR resonances of compound **16** are shown (with the exception that P1 CH<sub>2</sub> is of DDIVPC) when free (colored blue) and after adding small amounts of NS3 protease (colored red). (c) A comparison of free-state (ROESY NMR) versus bound-state (tr-NOESY) conformation and dynamics. Note the similarities of the backbone and differences of the side-chains. (d) Inhibitor **16** is shown with its inhibition constant and free-state <sup>13</sup>C T<sub>1</sub> relaxation times (next to each carbon). The amino acid positions are designated on top as P6–P1. The inhibition constant was determined using an assay involving the NS3 protease domain and an NS4A peptide [44]. <sup>13</sup>C T<sub>1</sub> relaxation data are given next to each protonated carbon. In cases where a carbon has more than one covalently attached hydrogen, NT<sub>1</sub> values are provided, where N is the number of attached protons and NT<sub>1</sub> is the product to help in interpreting the relative flexibility between different carbon types. Reproduced with kind permission from Springer Science + Business Media: *Top. Curr. Chem.*, Exploiting Ligand and Receptor Adaptability in Rational Drug Design Using Dynamics and Structure-Based Strategies, 272, 2007, 287, Steven R. LaPlante, Figure 20.

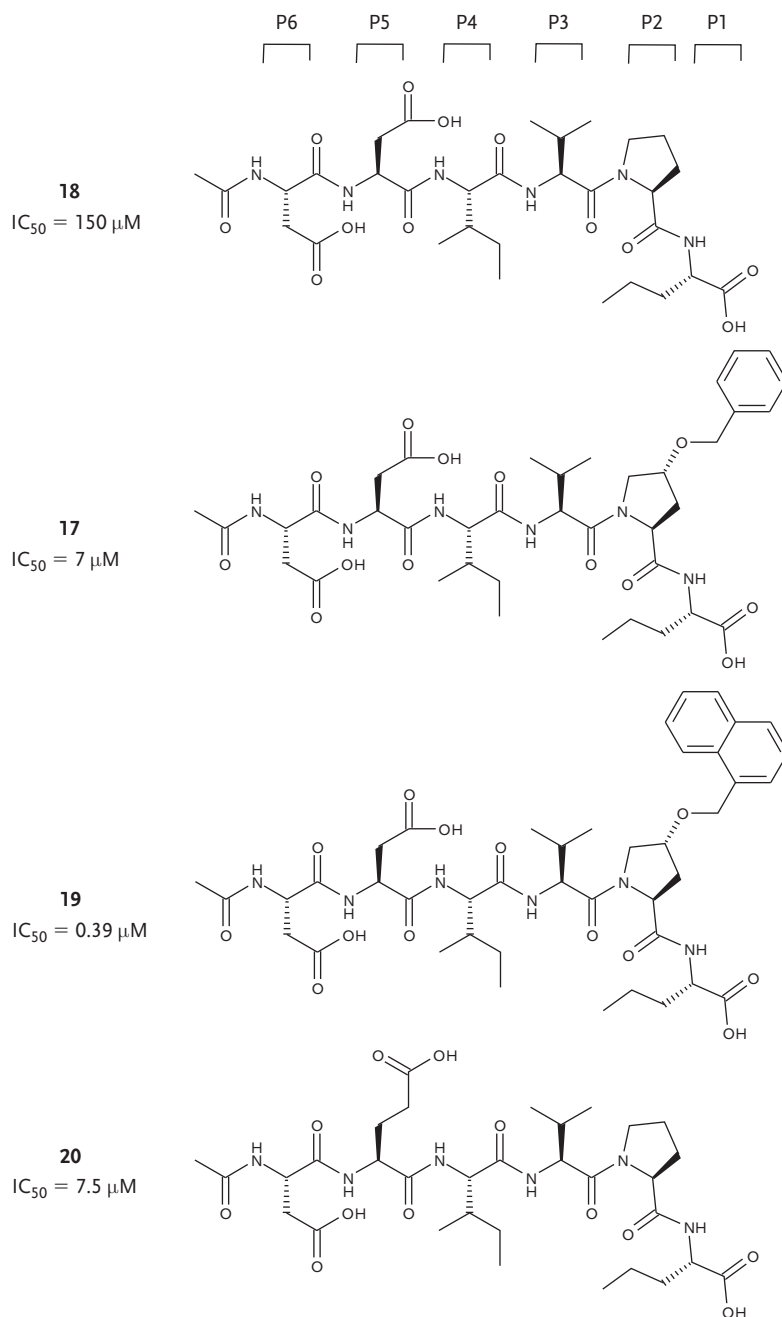


**Figure 1.11** Inhibitors 17–21 with inhibition constants determined using an assay that included the NS3 protease domain and an NS4A peptide [44]. The amino acid positions are designated on top as P6–P1.

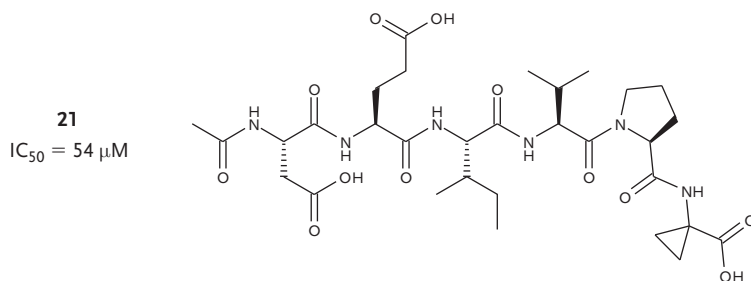


**Figure 1.11** (Continued)

was probed using an NMR ROESY experiment (Figure 1.10c) [43]. This comparison of the distance-related cross-peaks indicated that compound **16** adopts an extended backbone conformation in both states, with important differences observed for the side-chains.

A better means of monitoring dynamic attributes was sought and led the researchers to consider  $^{13}\text{C}$  NMR spin–lattice relaxation experiments ( $^{13}\text{C}$   $T_1$ ) [43].  $^{13}\text{C}$   $T_1$  relaxation is sensitive to segmental flexibility in the picosecond to nanosecond timescales, and the internal flexibility of drug-like ligands in the free state, which influences the binding affinity to macromolecules via entropic costs, typically occurs within these timescales. The direct correlation of  $^{13}\text{C}$   $T_1$  relaxation data with molecular flexibility can be made qualitatively for protonated carbons of free ligands where longer relaxation times are generally indicative of increased segmental flexibility [20, 43].

This work indicated that segmental fluctuations of the norvaline group in the free state was evident given the long and incremental increases of  $^{13}\text{C}$   $T_1$  times for the  $\alpha$  to  $\delta$ -carbons (Figure 1.10d,  $\alpha$  0.39,  $\beta$  0.60,  $\gamma$  0.94, and  $\delta$  3.66 s). Thus, it was reasoned that P1 replacements, which chemically rigidify this side-chain to resemble the bound conformation shown in Figure 1.10a, would likely be more potent owing to a lower entropic cost of binding.

The P2 substituent of **17** also exhibited significant flexibility in the free state, indicating that this aromatic ring underwent fast rotation or spinning along the benzylic/para-carbon axis. Replacement of the phenyl group with a larger naphthyl resulted in an 18-fold improvement in potency (compare compounds **17** and **19**, Figure 1.11) [44], which is likely due, in part, to a reduction in rotational rate and the associated entropic cost of binding (*vide infra*).

The ensemble of data in Figure 1.10 revealed features relevant to the role of P3 for potency. The P3 side-chain played an indirect role in the binding affinity by sterically rigidifying the P3 backbone in the free state to resemble that of the bound extended conformation [20, 43, 45], as was found for the HCMV protease inhibitors. The P3 side-chain had no DLB (Figure 1.10b, and blue-colored hydrogens in Figure 1.10a) indicating that it had no direct binding to the pocket, despite the fact that its removal resulted in significant loss in potency. Thus, given the similarities, and as exploited in the HCMV program, it was suggested to again replace the P3 side-chain with a bulky *tert*-butyl side-chain (*vide infra*).

## 1.4.6

**N-Terminal Truncation and Improved P1, P2 and P5 Substituents**

DLB and transferred NOESY mapping suggested that the principle binding residues spanned P4–P1. At first, this appeared to contradict earlier attempts to reduce the size of non-optimized hexapeptides by the removal of N-terminal residues. This resulted in shorter peptides with no significant activity. However, a similar exercise was successful by first improving the potency of the hexapeptide series, to better anchor the inhibitor, using beneficial P1, P2, and P5 replacements [44]. For example, 21- and 384-fold improvements were observed when the P2 proline was substituted with a benzyl-methoxyproline (compound **17** versus **18**, Figure 1.11) and a naphthyl-methoxyproline (compound **19** versus **18**, Figure 1.11), respectively. A further threefold improvement in potency was observed when the P1 norvaline was replaced with a 1-aminocyclopropyl carboxylic (ACCA) (compound **21** versus **20**, Figure 1.11). Replacement of the P5 L-aspartic acid with a D-glutamic acid resulted in a 20-fold gain in affinity (compound **20** versus **18**, Figure 1.11) [44]. Combining these substitutions simultaneously into a single hexapeptide, resulted in an inhibitor with an  $IC_{50}$  of 0.013  $\mu$ M (compound **22**, Figure 1.12) [44].

This potent compound then served as the starting compound for a renewed effort at N-terminal truncation. Removal of the P6 residue and the P5 amide resulted in a 69-fold loss in potency (compound **23** versus **22**, Figure 1.12) and a tetrapeptide having a simple acetyl capping group resulted in a loss in affinity by 269-fold (compound **24** versus **22**, Figure 1.12) [44]. As a result, N-terminal truncation successfully resulted in tetrapeptides that had measurable activity, and that were also more drug-like. The affinity imparted by the P2 naphthyl methoxy and P1 ACCA likely also helped to “anchor” the C-terminal end in the bound state.

Further improvements in potency were sought. It was found that an ethyl appendage on the P1 ACCA provided beneficial contributions to potency (compound **26** is twofold more potent than compound **24**, Figure 1.13) and further improvements could be gained by a vinyl appendage (compound **27** is 12-fold more potent than compound **24**) [46]. The requirement for a specific stereochemistry of the appendage was observed, given that a fourfold loss in affinity was measured for compound **25** as compared to **24** (Figure 1.13). Overall, it is noteworthy that the P1 ACCA group both improved potency and had a more rigidified, bioactive conformation in the free state as compared to the more flexible P1 Nvl (Figure 1.10d). Like P2, the P1 position played multiple roles in the bimolecular interaction. Due to these multiple roles, “sensemaking” exercises were required to qualitatively deconvolute the roles as much as possible, allowing further exploitation.

A combinatorial chemistry approach was also undertaken to identify alternative P2 substituents [48]. A large variety of aromatic groups was appended to the oxy-prolyl group at P2, resulting in two promising lead compounds **28** and **29** (Figure 1.14). The bound structure of each compound was then determined by transferred NOESY and conformational search methods [49]. These structures are

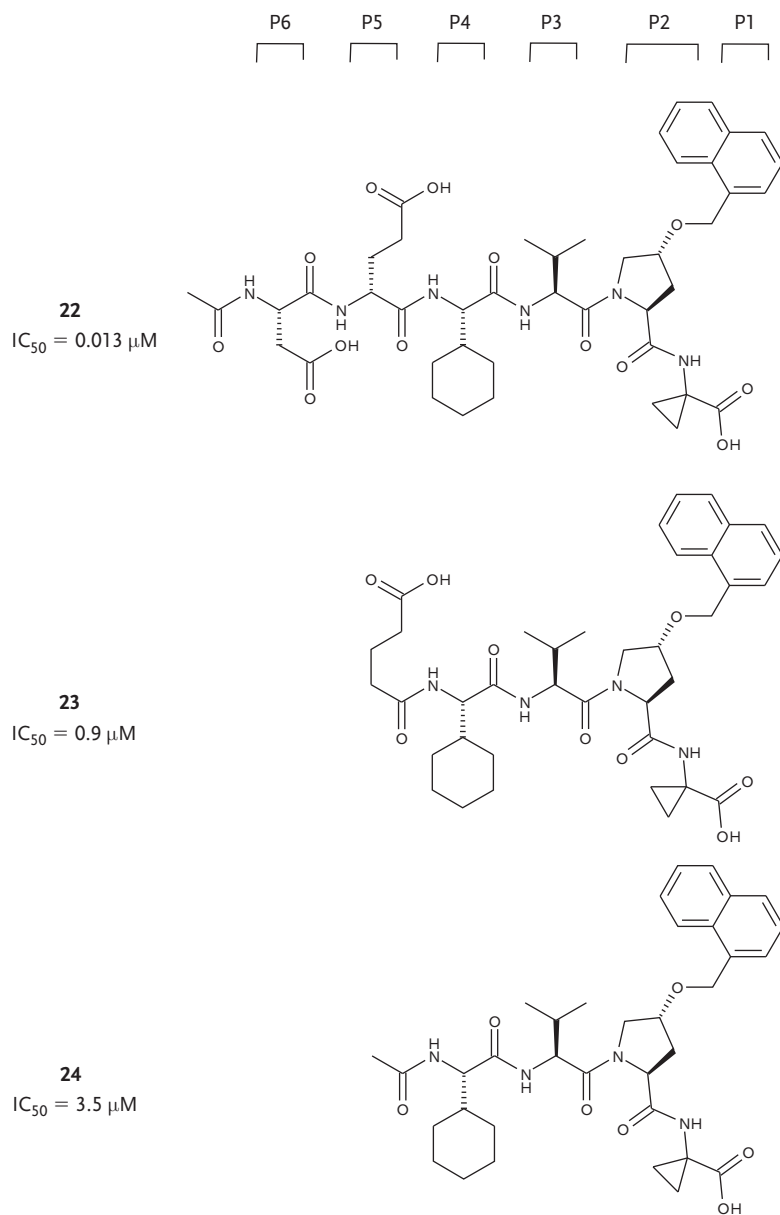


**Figure 1.12** Inhibitors **22–24** with inhibition constants determined using an assay that included the NS3 protease domain and an NS4A peptide [44]. The amino acid positions are designated on top as P6–P1. Reproduced with kind permission from Bentham Science Publishers Ltd.: *Curr. Med. Chem. – Anti-Infective Agents, Dynamics and Structure-based Design of Drugs Targeting the Critical Serine Protease of the Hepatitis C Virus – From a Peptidic Substrate to BILN 2061*, 4, 2005, 119, Steven R. LaPlante and Montse Llinàs -Brunet, Figure 7.

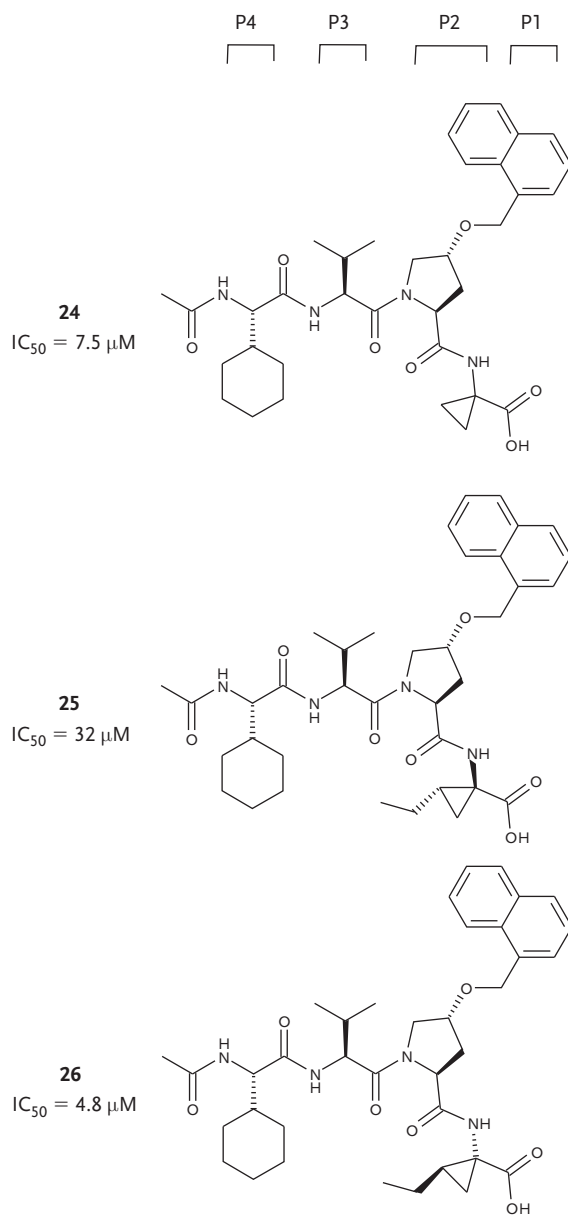


**Figure 1.13** Inhibitors **24–27** with inhibition constants determined using an assay that included the full-length NS3–NS4A protein [46, 47]. The amino acid positions are designated on top as P4–P1.

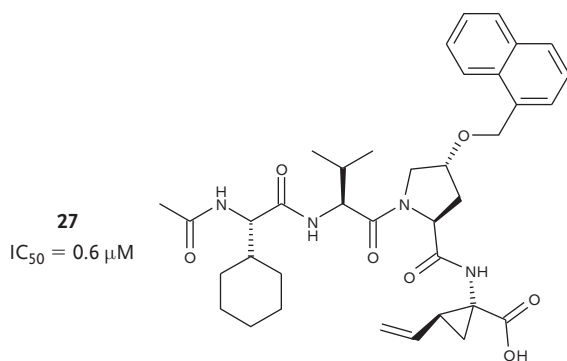


**Figure 1.13** (Continued)

shown on the right in Figure 1.14. Given that the biphenyl group of compound **29** and the quinoline ring of compound **28** occupy different physical space when bound to NS3 protease, it was hypothesized that a compound having three rings would better span both regions of space and could result in an improved affinity (see the theoretical superposition of compounds **28** and **29** on the right of compound **30**). A >10-fold improvement in potency was observed (compound **30**), but transferred NOESY data for a compound related to **30** showed that the tricyclic group actually bound in the opposite orientation from that predicted. This was understood when considering the multiple roles played by the P2 substituent (*vide infra*), including its effect on free-state rigidification, solvent shielding of the catalytic triad and electrostatic interactions.

#### 1.4.7

##### Macrocyclization: Linking the Flexible P1 Side-Chain to P3

At this stage of the project, the following considerations were given to improving the properties of the series. The transferred NOESY model of the complex involving compound **16** (Figure 1.10a) revealed that the P3 side-chain lies on the solvent-exposed surface of the protease and in close proximity to the P1 norvaline side-chain [43, 50]. Transferred  $^{13}C$   $T_1$  data (Figure 1.10a) indicated that the P1 side-chain underwent rigidification upon binding the protease [51]. It was speculated that intramolecular linking of the P1 side-chain to the P3 side-chain with a hydrocarbon bridge would lead to a macrocyclic inhibitor which would, in the free state, preferentially adopt the bound conformation observed for compound **16** in Figure 1.10a. A rigid macrocyclic scaffold would also ensure that the P2–P3 amide bond would adopt exclusively the trans-geometry observed in the bound conformation, unlike linear peptides which exist as a mixture of cis- and trans-rotamers.

As an example of the impact that macrocyclization can have on potency [50] and free-state flexibility, the macrocyclic compound **32** in Figure 1.15 (15-membered

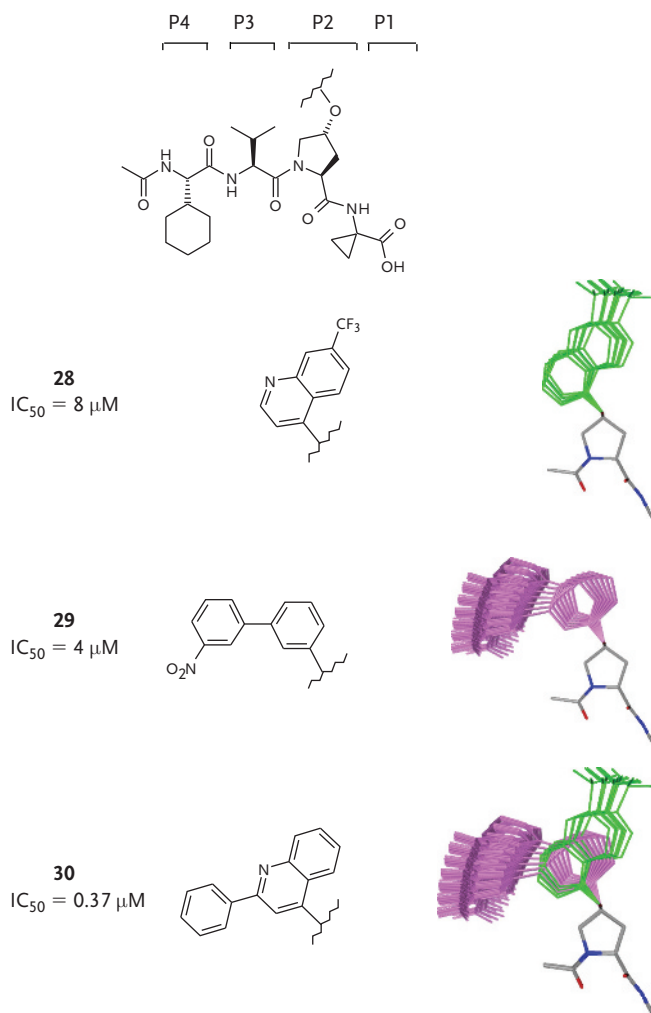


**Figure 1.14** Inhibitors **28–30** with inhibition constants determined using an assay that included the NS3 protease domain and an NS4A peptide [40, 49]. The amino acid positions are designated on top as P4–P1. The protease-bound structures of inhibitors **28** and **29** are provided on the right and were determined using transferred NOESY data and a conformational search protocol. Both are overlaid on the right of inhibitor **30** to illustrate the design concept. Reproduced with kind permission from Bentham Science Publishers Ltd.: *Curr. Med. Chem.* – Anti-Infective Agents, Dynamics and Structure-based Design of Drugs Targeting the Critical Serine Protease of the Hepatitis C Virus – From a Peptidic Substrate to BILN 2061, 4, 2005, 122, Steven R. LaPlante and Montse Llinàs-Brunet, Figure 10.

ring) is 10-fold more potent than the acyclic compound **31**. <sup>13</sup>C T<sub>1</sub> data are shown for both compounds in Figure 1.15, indicating that a reduction in the flexibility of the P1 side-chain (cyclopropyl and vinyl) was achieved by macrocyclization, as shown by the shorter <sup>13</sup>C T<sub>1</sub> relaxation times for this residue in compound **32**

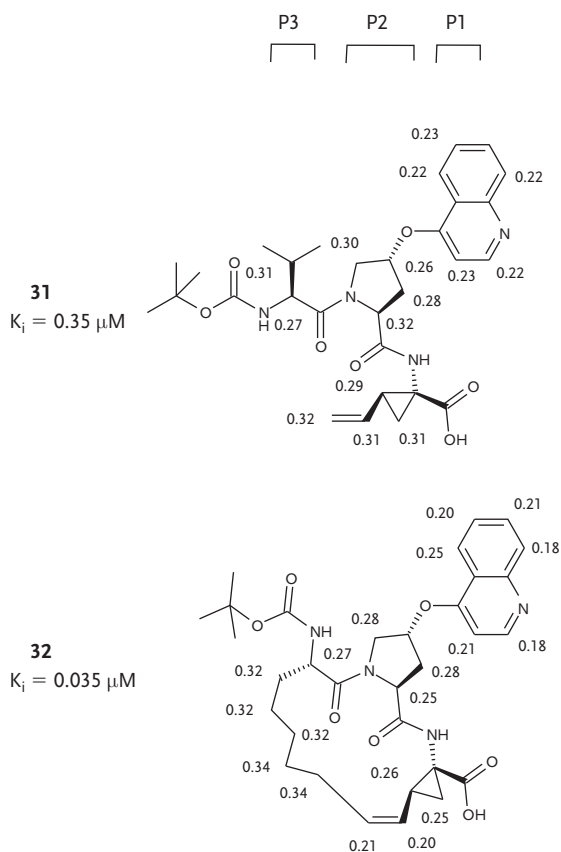


**Figure 1.15** Inhibitors **31** and **32** with inhibition constants determined using an assay that included the full-length NS3–NS4A protein. The amino acid positions are designated on top as P3–P1. The free-state  $^{13}\text{C}$   $NT_1$  relaxation times are also provided next to each carbon position (see also the legend of Figure 1.10). Reproduced with kind permission from Bentham Science Publishers Ltd.: *Curr. Med. Chem. – Anti-Infective Agents, Dynamics and Structure-based Design of Drugs Targeting the Critical Serine Protease of the Hepatitis C Virus – From a Peptidic Substrate to BILN 2061*, 4, 2005, 123, Steven R. LaPlante and Montse Llinàs-Brunet, Figure 12.

(Figure 1.15, 0.21–0.26 s) as compared to the acyclic compound **31** (Figure 1.15, 0.29–0.32 s).

The employed strategies described above [40–57] included an early “sensemaking” and knowledge building phase in which structural and dynamics data were acquired to, (i) understand the bioactive conformation of lead peptides when bound to HCV protease, (ii) identify the important substituents that directly contact the protease pocket, and (iii) determine the differences in conformational flexibility between the free and bound states of ligands. With the rational use of this information, medicinal chemists identified potent hexapeptide compounds

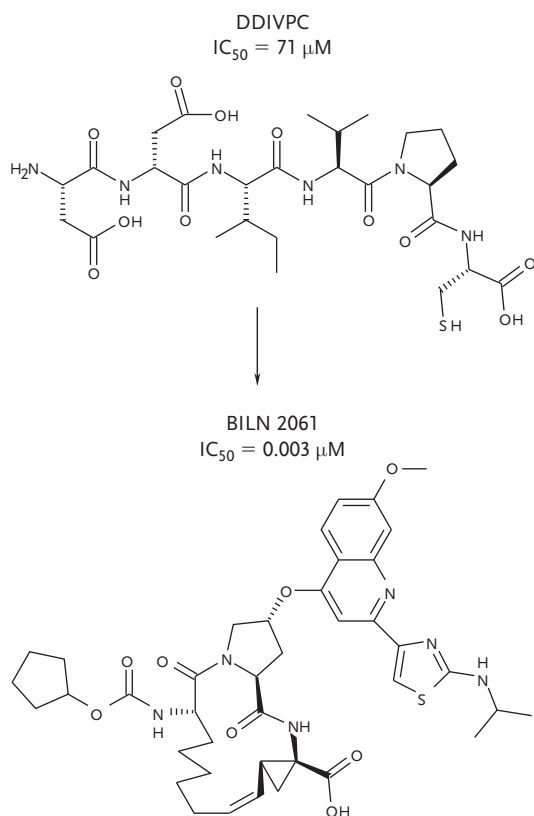


**Figure 1.16** Structures of the lead peptide DDIVPC and the clinical compound BILN 2061. Reproduced with kind permission from Springer Science + Business Media: *Top. Curr. Chem.*, Exploiting Ligand and Receptor Adaptability in Rational Drug Design Using Dynamics and Structure-Based Strategies, 272, 2007, 278, Steven R. LaPlante, Figure 14.

with improved P1, P2, and P5 substituents. Efforts to reduce the size and peptidic character resulted in N-terminal truncation to tetra- and tri-peptidic compounds that had novel P1 and P2 substituents. The macrocyclic scaffold was then designed to chemically rigidify the free-state conformation to further resemble the bound-like state, which resulted in a reduction in entropic costs of binding. Having extensive information regarding the binding mode of compounds, medicinal chemists exploited this knowledge in their campaign that eventually led to the BILN 2061 family of compounds. Further SAR efforts at P2 and P4 delivered the first clinical candidate **BILN 2061** (ciluprevir) [58, 59] which was the first compound to show proof of concept in humans for a direct acting anti-HCV protease inhibitor, see Figure 1.16. However, the further development of this compound was discontinued due to the observation of cardiotoxicity in high-dose monkey toxicology studies.

## 1.4.8

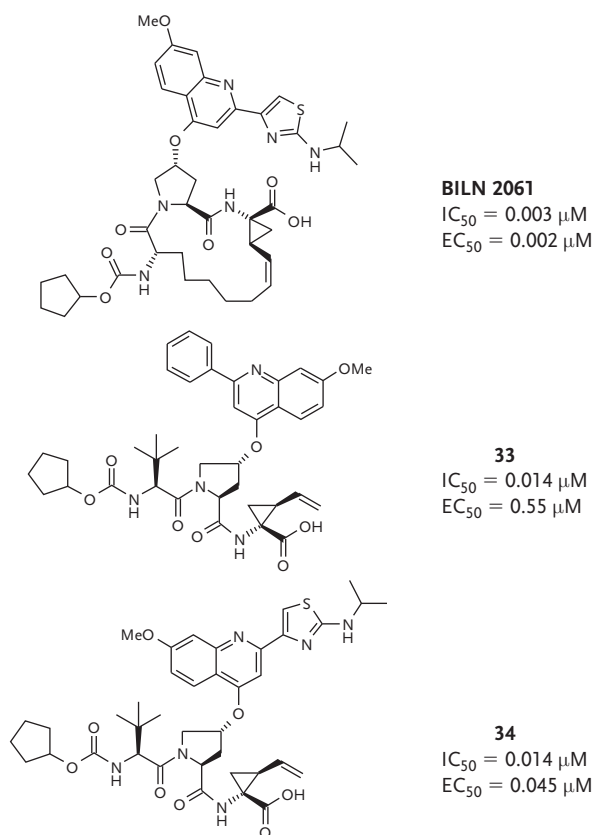
**HCV Protease Inhibitor BI00201335**

With the discovery of cardiotoxicity and subsequent discontinuation of development of the HCV NS3 protease inhibitor **BILN 2061** [55], this caused a re-evaluation of active material within the project in an effort to discover novel, non-covalent NS3 protease inhibitors [60].

Work continued on the C-terminal carboxylic acid, (1*R*,2*S*)-1-amino-2-vinyl-cyclopropyl carboxylic acid (vinyl-ACCA)-containing inhibitors [46], as these features provided good potency, excellent selectivity, as well as better solubility than seen with other classes of inhibitors. An advantage of a related linear series of inhibitors [52] lies in the fact that the synthetic complexity and costs associated with drug production are significantly reduced. These points taken together, the project then focussed on merging the SAR of both linear and macrocyclic series of inhibitors [61]. First, the quinoline moiety of **BILN 2061** was cross-fertilized with the linear derivative **33**, providing compound **34** (Figure 1.17) which displayed more than a 10-fold improvement in potency in the replicon assay [61]. This provided the first linear tripeptide inhibitor in our program with cellular activity below 100 nM [61].

Cell-based activity of this linear series needed to be improved whilst concomitantly evaluating and improving its ADME/PK profile. Compound **34** was used as the starting point for further evaluation. From this point in the project, the peptide backbone was retained, as this makes optimal interactions with the enzyme which mimic the canonical substrate binding mode, with both the NH and CO groups of the P3 residue and the NH group of the P1 moiety being involved in key hydrogen bonds with the protein [52]. Additionally, both the vinyl-ACCA derivative at P1 and the *tert*-butyl glycine moiety at P3 were retained as they were found to be optimal. The C-terminal carboxylic acid makes key interactions with the catalytic triad and the oxyanion hole [50], providing good potency and specificity towards NS3 *versus* human and other serine proteases [41]. In addition, one clear advantage over the other classes of reported NS3 protease inhibitors is the observed increase in solubility for this series. The *tert*-butyl found at P3 was also maintained as this was found to rigidify the peptidic backbone and to favor the overall extended conformation, found in the bound state, for the inhibitor in solution [52]. Thus, the SAR focussed on optimizing both the capping group and the P2 aminothiazol-quinoline moiety. SAR at P2 indicated the acetyl group, as in compound **35**, was well tolerated and increasing the size resulted in a loss of potency (Table 1.1). Further substitution on the quinoline core provided compounds **36** and **37** (Table 1.1), both displaying EC<sub>50</sub> values <20 nM in the replicon assay and these compounds were further improved to compounds **38–40**, Table 1.1. Combining double quinoline-core substitutions with variation of the aminothiazole-acyl group led to **BI00201335**, Table 1.1, which contains a highly optimized peptide backbone, as well as a C-terminal carboxylic acid and large P2 substituent. **BI00201335** has low nM activity in enzymatic and cellular assays, see Table 1.1.

This compound possessed favorable properties, as exemplified by pharmacokinetic parameters in rats, see Table 1.2, is selective in a large panel of human

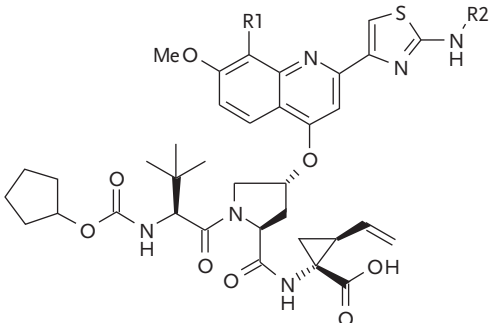


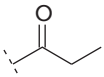
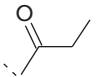
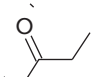
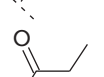
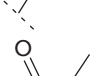
**Figure 1.17** Linear tripeptide HCV NS3 protease inhibitors. Reprinted with permission from *J. Med. Chem.*, 2010, 53, 6466-6476 (Table 1) Discovery of a potent and selective noncovalent linear inhibitor of the hepatitis C virus NS3 protease (BI 201335). Llinàs-Brunet, M., Bailey, M.D., Goudreau, N., Bhardwaj, P.K., Bordeleau, J., Bös, M., Bousquet, Y., Cordingley, M.G., Duan, J., Forgione, P., Garneau, M., Ghire, E., Gorys, V., Goulet, S., Halmos, T., Kawai, S.H., Naud, J., Poupart, M.-A., White, P.W. Copyright 2010 Americal Chemical Society.

proteases and is currently in phase III clinical trials. The genesis of this compound owes its existence to the careful inhibitor design of progenitor macrocyclic and linear series, along with the transfer of “sensemaking” lessons from the earlier HCMV program, *vide supra*, and illustrates that peptides can be de-peptized and turned successfully into clinical candidates.

In HCV-infected patients, an impressive (average) viral load decrease of  $-5.3 \log_{10}$  has been seen with a 240 mg qd dose of **BI00201335** in combination with pegylated Interferon- $\alpha$  and ribavirin over 28 days of treatment, see Figure 1.18 [62]. No viral breakthroughs were observed for the six patients treated under this regime.

In conclusion for these two targets, this work has the distinction of systematically monitoring the structure and dynamics features of ligands using

**Table 1.1** Optimization of linear tripeptide NS3 HCV protease inhibitors.


Compound	R1	R2	IC <sub>50</sub> (nM)	EC <sub>50</sub> (nM)
35	H		5	34
36	Me		8	19
37	Me		10	17
38	F		7	36
39	Cl		7	11
40	Br		7	5
BI00201335	Br		3	3

**Table 1.2** Pharmacokinetic parameters of BI00201335 in rats following oral and intravenous administration.

Compound	Oral 5 mg/kg		i.v 2 mg/kg			
	C <sub>max</sub> (μM)	AUC <sub>0-∞</sub> (μM h)	T <sub>1/2</sub> (h)	V <sub>ss</sub> (L/kg)	Cl (mL/min/kg)	F%
BI00201335	0.6	1.7	1.2	1.9	20	40

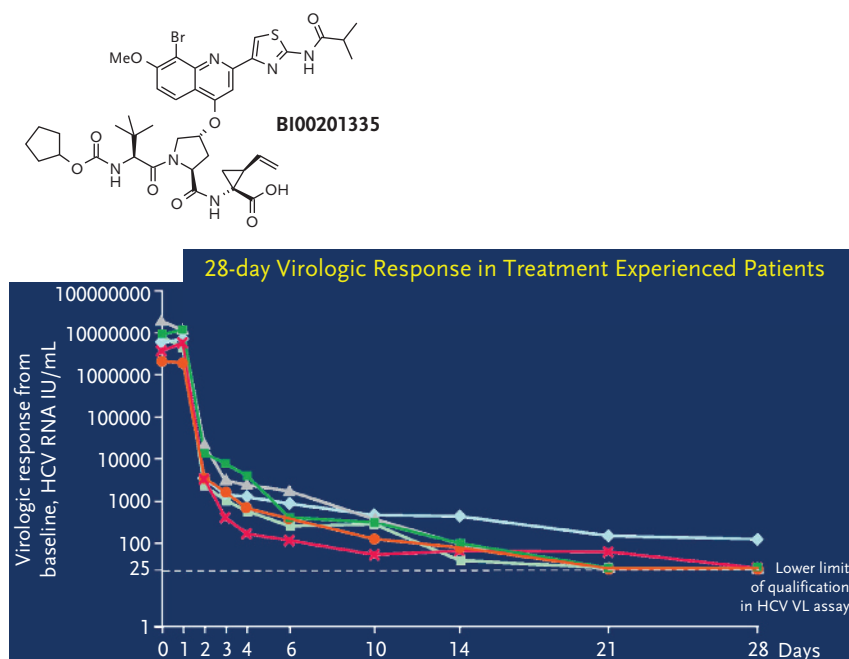


**Figure 1.18** Structure of BI00201335 and viral load decline in patients.

multidisciplinary strategies. It is certain that the well-characterized systems described here are not unique and that most bi-molecular interactions involve a range of adaptive processes. The simplistic “lock-and-key” and “induced-fit” views of ligand binding must evolve to a better understanding of intermediate events and properties. The work described here can serve as an example for monitoring and exploiting adaptive features.

## 1.5

### Herpes Simplex Virus

#### 1.5.1

##### Herpes Simplex Virus-Encoded Ribonucleotide Reductase Inhibitors

Herpes simplex viruses (HSV-1 and HSV-2) are responsible for a number of human diseases, such as genital and oral lesions, ocular disease, and encephalitis. HSV encoded the enzyme ribonucleotide reductase (RR) which is responsible for the conversion of ribonucleoside diphosphates into the corresponding 2'-deoxyribonucleotides. As RR is an essential viral pathogen, a selective RR inhibitor is an attractive target for drug development. HSV RR is composed of two distinct homodimeric subunits [63, 64]. Association of these two subunits is

essential for catalytic activity, and the C-terminus of the smaller of the two subunits is critical for association [65]. When this small subunit lacks seven amino acids at the C-terminus, it does not bind to the larger subunit [66] and catalytic activity is lost. Peptides and peptide mimetic inhibitors of this region have been investigated as a route to new drug design [66–70].

NMR studies found that the last 32 amino acid residues of the C-terminus of R2 are disordered [71]: A published X-ray structure of *E.coli* RR R2 [72] was consistent with this, and also suggested that this region was disordered (no electron density was observed). It is important to determine this to understand whether conformationally-constrained inhibitor design would work. Researchers found that the last six amino acids are more mobile than the rest of the protein, that these amino acids are conformationally similar to the corresponding amino acids of the 15-amino acid analogous peptide and that this corresponds to the critical binding region of the C-terminus responsible for subunit recognition. Critically, the researchers found that it was not necessary to study the small subunit C-terminus further and that conformational analysis of C-terminal peptides and their derivatives could be sufficient to gain insight into the bioactive conformation.

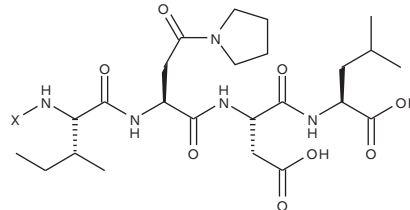
Knowledge of the bound conformation of peptides to the large subunit was then sought [70]. It was known that the nonapeptide H-Tyr-Ala-Gly-Ala-Val-Val-Asn-Asp-Leu-OH **41** corresponds to the nine C-terminal amino acids of the HSV RR small subunit and that this inhibits HSV RR with an IC<sub>50</sub> of 38 μM by preventing subunit association, see Table 1.3. It was desired to use **41** as a starting point to further improve inhibitor potency and reduce its size. The first tactic undertaken was to truncate the peptide at the N-terminus by up to four amino acids in **41** and this still provided inhibitors with some level of activity: compound **42** has an IC<sub>50</sub> of 760 μM against HSV RR [65, 73]. It was deduced that peptide **42** contained the minimum structural requirements for binding to the large subunit. SAR continued on analogs of this peptide **42**.

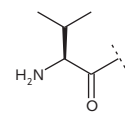
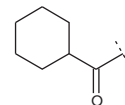
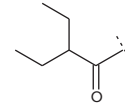
Earlier SAR had established that replacement of the asparagine side-chain NH<sub>2</sub> with a pyrrolidine provided a 50-fold boost in potency (**43**; IC<sub>50</sub> 13 μM), see Table 1.4 [72]. This potency boost was necessary to undertake meaningful SAR studies and **43** was used as the basis for SAR investigations.

**Table 1.3** Truncation of nonapeptide to minimum active fragment.

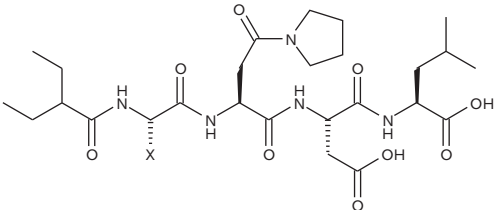
	Compound	IC <sub>50</sub> (μM)
41	H-Tyr-Ala-Gly-Ala-Val-Val-Asn-Asp-Leu-OH	38
	H-Ala-Gly-Ala-Val-Val-Asn-Asp-Leu-OH	280
	H-Gly-Ala-Val-Val-Asn-Asp-Leu-OH	220
	H-Ala-Val-Val-Asn-Asp-Leu-OH	190
42	H-Val-Val-Asn-Asp-Leu-OH	760
	H-Val-Asn-Asp-Leu-OH	> 2000
	H-Tyr-Ala-Gly-Ala-Val-Val-Asn-Asp-OH	> 2000

Table 1.4 Modifications at the N-terminus

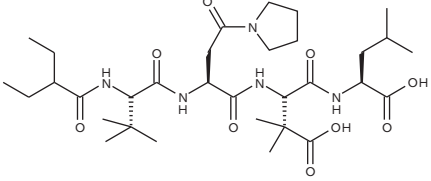


Compound	X	IC <sub>50</sub> (μM)
43		13
44		> 1000
45		1.5
46		1.5

Moving from the N-terminus to the C-terminus and optimizing substituents at each position before incorporating this optimized substituent into the optimization of the following round for the next substituent, we see that the capping group for the N-terminus supports lipophilic groups, with the simple acetyl compound being essentially inactive (**44**; IC<sub>50</sub> > 1000 μM), Table 1.4, whereas the cyclohexylamine (**45**; IC<sub>50</sub> 1.5 μM) and the diethylacetyl-chain (**46**; IC<sub>50</sub> 1.5 μM) were equally active. The latter is smaller and less lipophilic and so was taken forward into the next design round. Modifying the Ile-side chain led to compound rigidification by incorporation of a *tert*-butyl group, see Table 1.5 (**47**; IC<sub>50</sub> 0.6 μM), forcing the inhibitor to access the bioactive conformation. Compare this to the simple methyl **48** and proton compounds **49** that are less active. It is noteworthy that this knowledge inspired the use of similar *tert*-butyl groups in the HCMV and HCV programs (*vide supra*). SAR of the asparagine position failed to improve potency over that achieved with the pyrrolidine substituent, whereas addition of a geminal-dimethyl group to the aspartic acid side chain improved potency further. Finally, modification of the C-terminal position confirmed that a substituted carboxylate at the aspartic acid position was the optimal group for potency, compound **50**.

**Table 1.5** Modifications leading to inhibitors accessing the bioactive conformation


Compound	X	IC <sub>50</sub> (μM)
46		1.5
47		0.6
48		11
49		77

50: IC<sub>50</sub> 0.18 μM

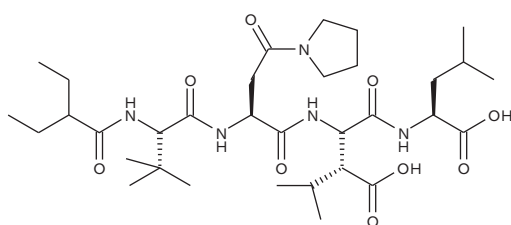
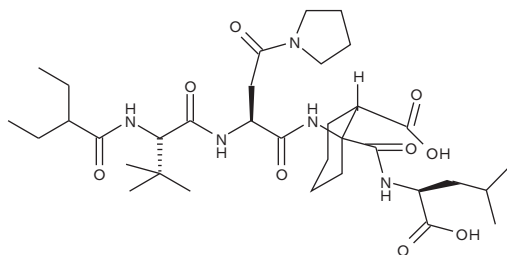
Compounds were tested for selectivity of HSV ribonucleotide reductase inhibition over human RR. Table 1.6 indicates that selectivity was maintained.

Thus, SAR studies led to the identification of a substituted tetrapeptide **50** with a 200-fold improvement in potency over the nona-peptide (**41** in Table 1.3) and >4000-fold more potent over the heptapeptide (**42** in Table 1.3). Further SAR studies provided **51**, Figure 1.19, [74] which has an (*s*)-isopropyl side chain on the aspartate group and provides a compound with an IC<sub>50</sub> of 8 nM. NMR studies confirmed the conformational preference in solution for these inhibitors. The orientation of the carboxylate group was profoundly affected by the beta-alkyl group. Based on these and other conformation preferences deduced from NMR studies, a conformational restriction approach was attempted, with some success. From these efforts, compound **52**, which possessed an IC<sub>50</sub> of 56 nM, was synthesized.

Further optimization of the aspartic acid side chain, this time to a cyclopentyl-side chain and isopropyl to *tert*-butyl side chain modification at the leucine residue and the N-terminal cap to a phenylethylacetyl group, provided **BILD 1257** (Figure 1.20: EC<sub>50</sub> 35 μM [HSV-1]; 30 μM [HSV-2]). However, compounds in this

**Table 1.6** Selectivity of HSV ribonucleotide reductase inhibition over human ribonucleotide reductase

Compound	IC <sub>50</sub> (μM)	
	HSV-RR	Human-RR
47	0.6	>1000
46	1.5	>1000
50	0.18	>1000

51: IC<sub>50</sub> 0.008 μM52: IC<sub>50</sub> 0.056 μM**Figure 1.19** HSV ribonucleotide reductase inhibitors.

series were not cell penetrant. Analogous to strategies in the HIV protease field, neutral or basic compounds showed higher cell penetration. In this HSV series of compounds, the C-terminal carboxylate was changed to a hydroxymethyl group, giving compound **BILD 1263** which possessed reasonable cellular potency (Figure 1.20: EC<sub>50</sub> 3.1 μM for HSV-1 and 4.2 μM for HSV-2).

These discoveries led to the discovery of **BILD 1263** as a topical treatment that was shown to reduce the severity and incidence of HSV-1-induced stromal keratitis and corneal neovascularization in a murine ocular model [75]. A combination of NMR and molecular mechanics models was used to suggest a potential 3D structure for the inhibitors in the bound state as matching that in solution. Figure 1.21 indicates the groups important for binding and orientation into the

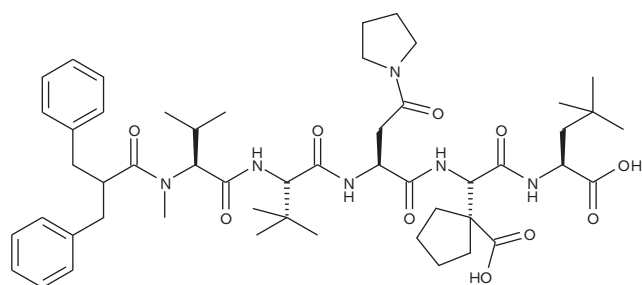


**BILD 1257:** EC<sub>50</sub> 35 μM (HSV-1)  
EC<sub>50</sub> 30 μM (HSV-2)

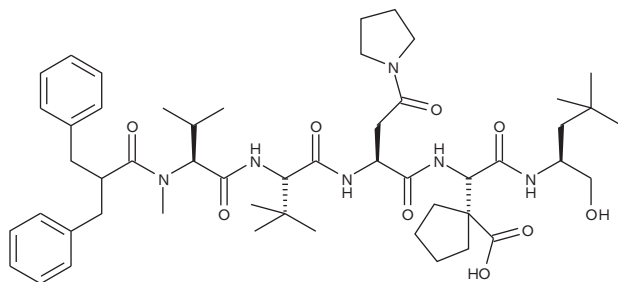


**BILD 1263:** EC<sub>50</sub> 3.1 μM (HSV-1)  
EC<sub>50</sub> 4.2 μM (HSV-2)

**Figure 1.20** Structures of advanced peptide mimics BILD 1257 and BILD 1263.

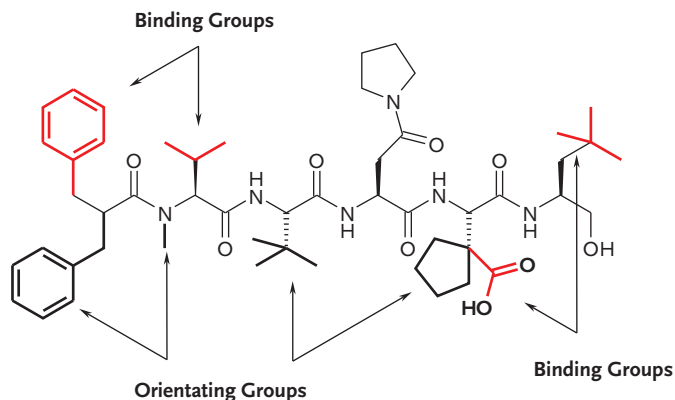


**Figure 1.21** Proposed 3D structure for the inhibitors in the bound state matching that in solution. Reprinted with permission from *J. Med. Chem.*, 1995, 38, 3617-3623 (Figure 2). Peptidomimetic Inhibitors of Herpes Simplex Virus Ribonucleotide Reductase: A New Class of Antiviral Agents. Moss, N., Beaulieu, P., Duceppe, J.S., Ferland, J.M., Gauthier, J., Ghio, E., Goulet, S., Grenier, L., Llinàs-Brunet, M., Plante, R., Wernic, D., Déziel, R. Copyright 1995 American Chemical Society.

bioactive conformation for peptide inhibitors. In the absence of X-ray information, correlation of potency with the structure of conformationally-restricted inhibitors has been undertaken to provide evidence of the bioactive conformation. Understanding an inhibitor's bioactive conformation and how the molecule binds to its target requires knowledge of what inhibitor functionalities are important for binding potency and why these are so.

A related target varicella zoster virus (VSV) RR is also inhibited by compounds in this series. The C-terminal sequence of VZV RR (YAGTVINDL) is similar to that of HSV RR (YAGAVVNDL) so it was reasoned that the same series of compounds could be active in both [76]. Table 1.7 gives the binding affinities of the nonapeptides corresponding to the C-terminal sequences of VZVRR and HSV RR (53 and 54, respectively). The peptides were reduced in size to find the minimum binding sequence to elicit activity, leading to compound 55 (Table 1.7: IC<sub>50</sub> of 4000 nM for HSV RR and 15000 nM for VZV) and compound 56 (Table 1.7: IC<sub>50</sub> of 24 nM for HSV RR and 588 nM for VZV). Following changes to the side chains to improve activity, compound 57 was obtained, Table 1.7, which possessed an IC<sub>50</sub> of 1 nM for HSV RR and 37 nM for VZV.

## 1.6

### Renin

#### 1.6.1

##### Aspartyl Protease Renin as a Target

Renin is an aspartyl protease that catalyzes the first rate-limiting step in the renin-angiotensin cascade [77]. Renin-angiotensin plays an important role in the regulation of blood pressure and the maintenance of sodium and volume homeostasis, where renin cleaves its substrate angiotensinogen (its only natural substrate) generating the decapeptide angiotensin I, which in turn is processed to the octapeptide angiotensin II by the angiotensin converting enzyme (ACE). Angiotensin II is a potent vasoconstrictor, therefore inhibitors of renin have been sought for the treatment of hypertension.

The potential of renin as a target has been recognized for decades but many potent peptides and peptidomimetics active against renin have displayed poor oral efficacy, attributed to poor absorption, a high first-pass clearance and/or proteolytic degradation.

A series of renin inhibitors, which are non-peptide inhibitors possessing a dipeptide replacement for the P<sub>2</sub>-P<sub>3</sub> segment (see Figure 1.22) was designed by researchers, as well as a known diol transition state analog, 4,5- and 3,5-dihydroxyhexanamide [78].

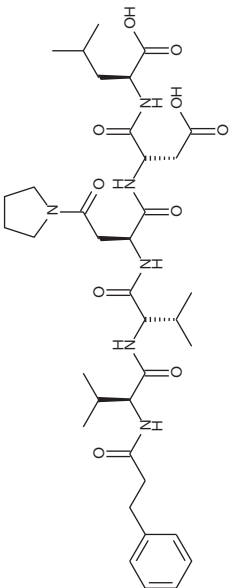
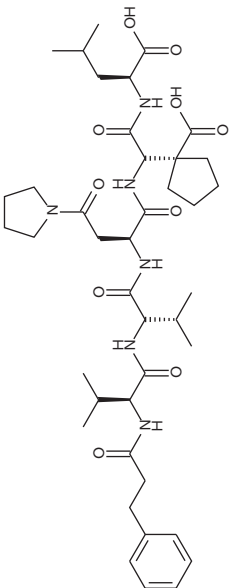
The inhibitors 58 and 59 span the P<sub>3</sub> P<sub>1</sub>' to positions and it had been shown that with renin inhibitors, the P<sub>3</sub> carbonyl interacts with the enzyme while the P<sub>2</sub>-P<sub>3</sub> amide NH forms a non-critical hydrogen bond [79]. The P<sub>2</sub>-P<sub>3</sub> replacements must achieve critical hydrogen bonds with the enzyme and orient the P<sub>3</sub> side chain whilst lacking the P<sub>4</sub> residue.

Table 1.7 Truncation of the nona-peptides corresponding to the C-terminal sequences of VZV RR.

Compound	Binding Assay IC <sub>50</sub> (nM)	
	HSV	VZV
53	8 000	11 000
54	25 000	42 000
55	4 000	15 000

(Continued)

Table 1.7 (Continued)

Compound	Binding Assay IC <sub>50</sub> (nM)		
	HSV	VZV	
56	24	588	
57	1	37	

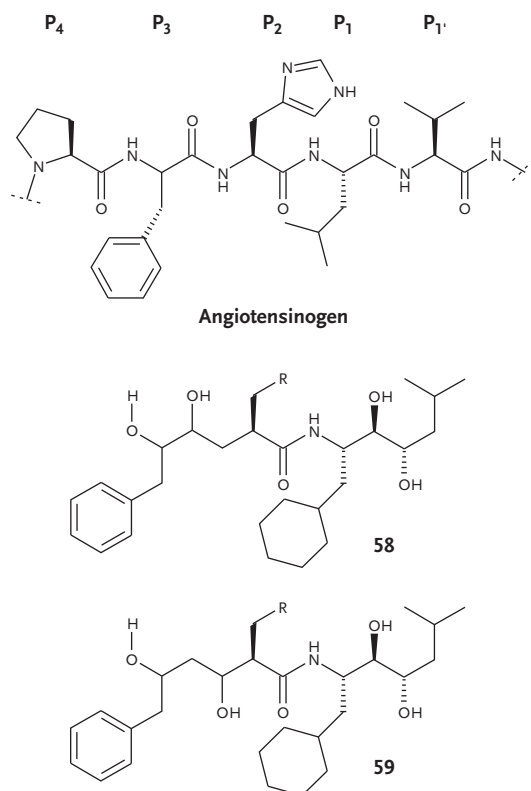


**Figure 1.22** Dipeptide replacement for the P<sub>2</sub>-P<sub>3</sub> segment of Renin and inhibitors spanning the P<sub>3</sub> to P<sub>1</sub>' positions of Renin. Reprinted from *Bioorganic & Medicinal Chemistry*, 6, Jung, G.L., Anderson, P.C., Bailey, M., Baillet, M., Bantle, G.W., Berthiaume, S., Lavallée, P., Llinàs-Brunet, M., Thavonekham, B., Thibeault, D., Simoneau, B., Novel Small Renin Inhibitors Containing 4,5- or 3,5-Dihydroxy-2-substituted-6-phenylhexanamide Replacements at the P<sub>2</sub>-P<sub>3</sub> Sites, 2317-2336 (Figure 2), Copyright 1998, with permission from Elsevier Science Ltd.

On route to optimizing this series of inhibitors, NMR spectroscopy was used to identify and compare the preferred solution conformations of the inhibitors [80]. Comparisons were also made between the unbound structures determined by NMR, and the renin-bound structures determined by X-ray crystallography [81].

Determination of solution conformations of inhibitors **60** to **62** (Figure 1.23a) in the unbound state indicated a major conformer for these inhibitors. By using NMR-derived restraints, the solution structures of the inhibitors were modeled using a combination of distance geometry, energy minimization, and molecular dynamics. The lowest 25 energy structures that satisfied the NMR data were superimposed (colored in black, Figure 1.23c). These were then compared with the crystal structures of renin complexed with inhibitors **60** to **62** [82], see the red

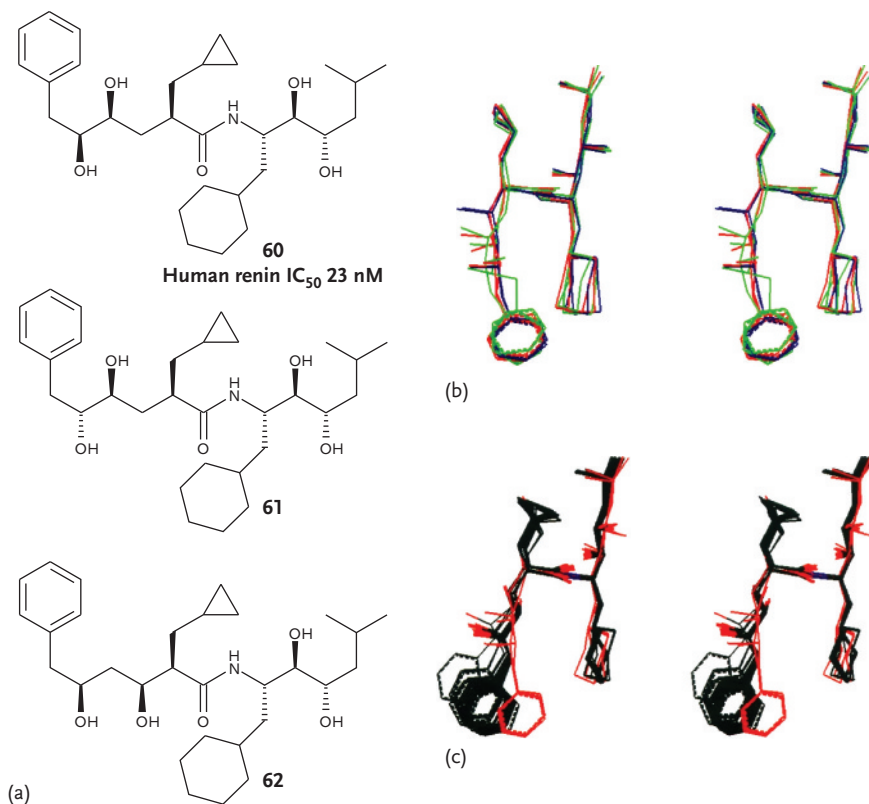


**Figure 1.23** Renin inhibitors. (a) structures of inhibitors **60–62**. (b) Stereoviews of the renin-bound structures of inhibitors **60–62** as determined by X-ray crystallography [82]. Inhibitors **60–62** are colored red, green and blue, respectively. Since there are two independent renin complexes per asymmetric unit, both forms for each inhibitor are shown. (c) Stereoviews of the solution structures of **60** (black) in the unbound state (determined by NMR) are shown superimposed with the renin-bound structures of **60** (red) (determined by X-ray crystallography).

colored structures in Figure 1.23c. As can be seen from Figure 1.23c, the inhibitors adopt similar conformations in the unbound and renin-bound states. Also, all three inhibitors have a similar overall conformation (Figure 1.23b), with the  $P_3$  showing the greatest variability. It was found that, although the inhibitors displayed similar conformations with renin-bound and unbound, the gross conformational changes of the inhibitor are not a prerequisite to binding renin. Differences were observed, for example, between the  $P_3$  position between inhibitors themselves and between renin-bound and unbound conformations. These differences were not detrimental to inhibitor potency.

Medicinal chemistry proceeded to attempt to optimize this series of peptidomimetics but this ultimately failed to deliver a series that was optimizable for

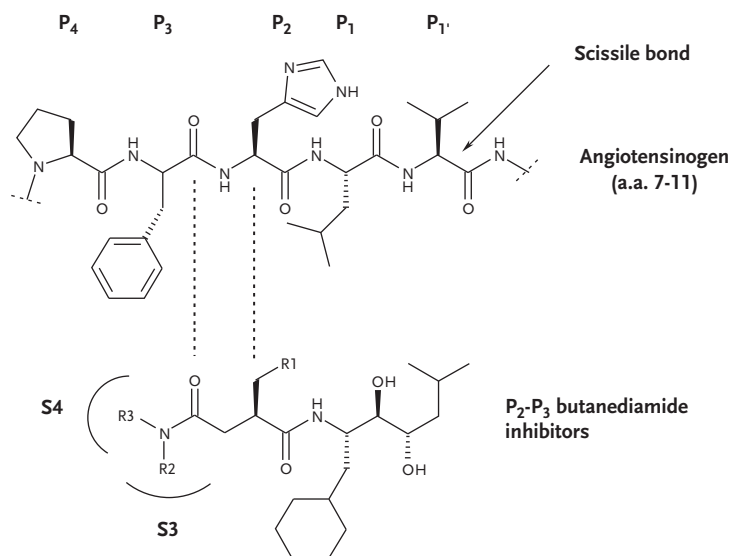


**Figure 1.24** Proposed P<sub>2</sub>-P<sub>3</sub> butanediamide inhibitors. Reprinted from *Bioorganic & Medicinal Chemistry*, 7, Simoneau, B., Lavallée, P., Anderson, P.C., Bailey, M., Bantle, G., Berthiaume, S., Chabot, C., Fazal, G., Halmos, T., Ogilvie, W.W., Poupart, M.-A., Thavonekham, B., Xin, Z., Thibeault, D., Bolger, G., Panzenbeck, M., Winquist, R., Jung, G.L., Discovery of non-peptidic P<sub>2</sub>-P<sub>3</sub> butanediamide renin inhibitors with high oral efficacy, 489-508 (Figure 1), Copyright 1999, with permission from Elsevier Science Ltd.

physicochemical properties, such as water solubility. One of the most promising compounds from this series was **60** which possessed an IC<sub>50</sub> of 23 nM, see Figure 1.23. [78].

Although potent (**60**: human plasma renin IC<sub>50</sub> 23 nM), inhibitors at this stage of the program lacked water solubility and so this series was abandoned in favor of a series where the focus for design was placed on the P<sub>2</sub>-P<sub>3</sub>-P<sub>4</sub> segment of the inhibitors [83] while maintaining a known transition state analog at P<sub>1</sub>-P<sub>1</sub>' [84].

Research centered around replacing the P<sub>2</sub>-P<sub>3</sub> peptide moiety with a butanediamide (Figure 1.24) as the NH at P<sub>2</sub> is not involved in an essential hydrogen bond it can, therefore, be replaced by a methylene. One stereogenic center is thus eliminated, leading to a decomplexation of overall structure. A medicinal chemistry program then followed to optimize potency and physico-chemical properties, varying substituents at P<sub>2</sub>-P<sub>3</sub>-P<sub>4</sub>. Optimization for potency at P<sub>1</sub> led to the introduction of a 2-amino-4-thiazolyl-group **63**, Figure 1.25; at P<sub>3</sub> to a cyclohexylmethyl substituent **64** and at P<sub>4</sub> to the introduction of an *N,N*-dimethylacetamide side chain **63**. Compound **63** was evaluated in a conscious sodium deplete cynomolgous monkey, given orally at a 10 mg/kg dose and this compound gave a statistically significant decrease in mean arterial blood pressure. Further

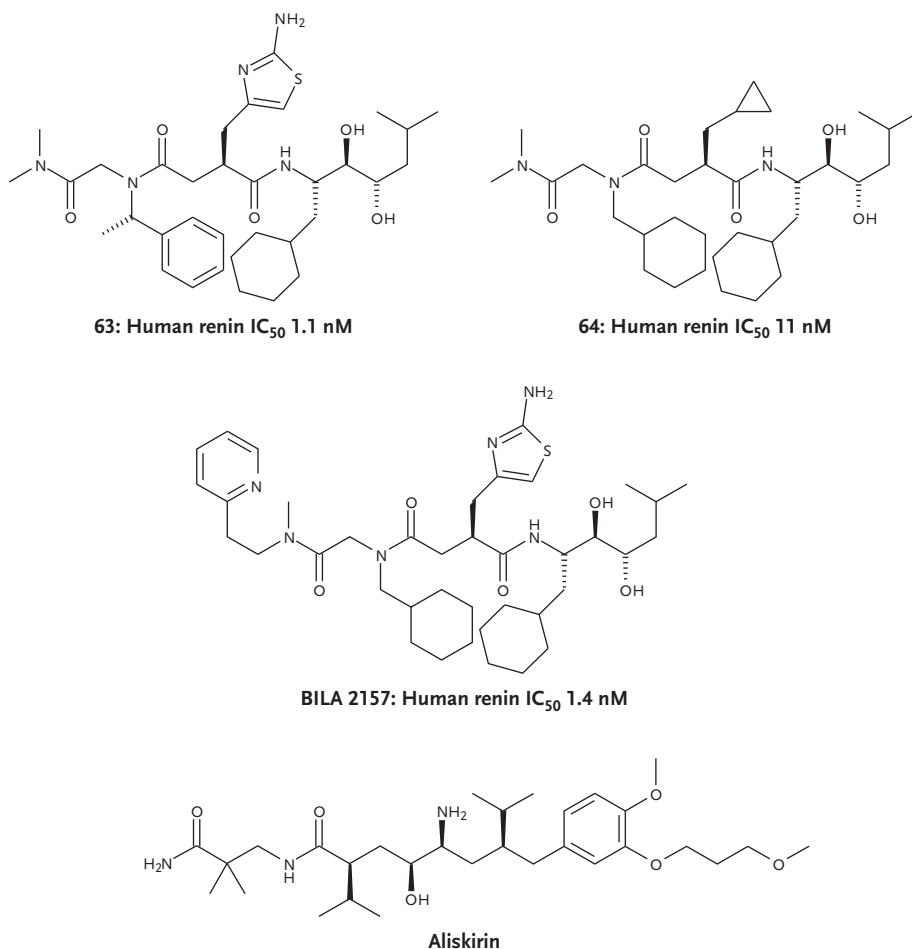


**Figure 1.25** P<sub>2</sub>-P<sub>3</sub> butanediamide Renin inhibitors.

optimization for compound **63** based on *in vivo* activity followed, focussing on the P<sub>4</sub> and P<sub>3</sub> positions by replacement of the *N,N*-dimethylamide fragment with an *N*-methyl-2-pyridylethyl-substituent. This compound **BILA 2157** was selected as the clinical candidate [85].

**BILA 2157** was potent, selective, possessed a simplified chemical structure and displayed a good oral activity of 40% in cynomolgus monkey, as well as displaying a statistically significant lowering of blood pressure in sodium-depleted animals, given at an oral dose of 3 mg/kg [83]. Further clinical development of this compound was stopped due to unforeseen toxicology observed in rats and dogs under chronic administration.

Some years later a related compound (Spp-100; Tekturna; Aliskirin<sup>®</sup>) was launched onto the market (see Figure 1.25).

## 1.7 HIV

### 1.7.1

#### HIV Protease Inhibitors

The human immunodeficiency virus (HIV) has been identified as the causative agent of acquired immune deficiency syndrome (AIDS). Studies of the virus' life-cycle have revealed a number of potential therapeutic intervention points: One of the most studied being the aspartyl protease enzyme of HIV, which has been shown to be essential for viral replication [86–89]. The enzyme is essential for processing the viral *gag* and *gag-pol* gene products through specific cleavage of peptide bonds [90–93]. The rational design of HIV protease inhibitors has relied upon the transition state mimic concept, applied to the cleavage of an amide bond. In this case, replacing an amide bond by a non-cleavable hydroxyethylamine dipeptide isostere, see Figure 1.26. In this way, a number of potent peptide-mimic viral replication inhibitors of the enzyme have been produced and made it to market [94, 95].

Originally, the highly peptidic nature of these HIV protease inhibitors resulted in limited oral bioavailability, short *in vivo* half-lives and complex structures [96]. From our own work aimed at simplifying the structure of HIV protease inhibitors, reducing the peptidic nature of the inhibitors as well as reducing charge and hydrophobicity, these efforts led to the synthesis of palinavir [97, 98] which contains a (*R*)-hydroxyethylamine transition state mimic and a novel 4-substituted pipercolic amide (see Figure 1.27). Palinavir is a highly potent and specific inhibitor of HIV-1 ( $EC_{50}$  4 nM) and HIV-2 proteases ( $EC_{50}$  10 nM), see Table 1.8 and Figure 1.27.

The bioavailability of palinavir in rats is 26%, significantly higher than that of Saquinavir (oral bioavailability 3%). Palinavir was nominated as the first clinical candidate against HIV protease (Figure 1.27), but development of this compound

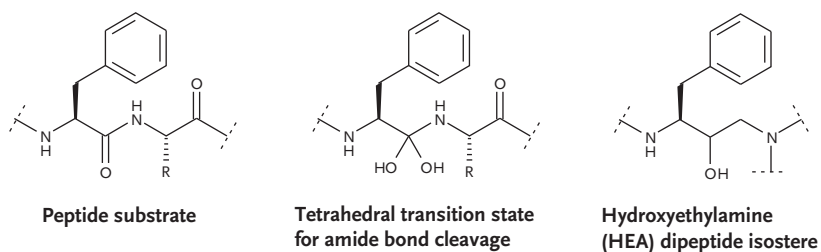
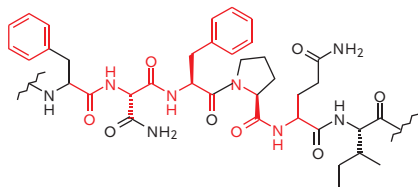
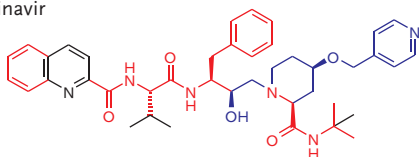


**Figure 1.26** Dipeptide isostere. Reprinted with permission from *J. Org. Chem.*, 1996, 61, 3635-3645 (Figure 1). Preparation of Aminoalkyl Chlorohydrin Hydrochlorides: Key Building Blocks for Hydroxyethylamine-Based HIV Protease Inhibitors. Beaulieu, P. and Wernic, D. Copyright 1996 American Chemical Society.

## Substrate sequence

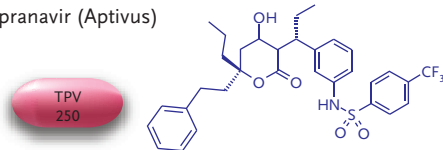


## Palinavir



- Peptidomimetic
- Stopped just before entering clinical phase

## Tipranavir (Aptivus)



- Non-peptidomimetic, potent against resistant mutants
- Approved by FDA in 2005
- On the market

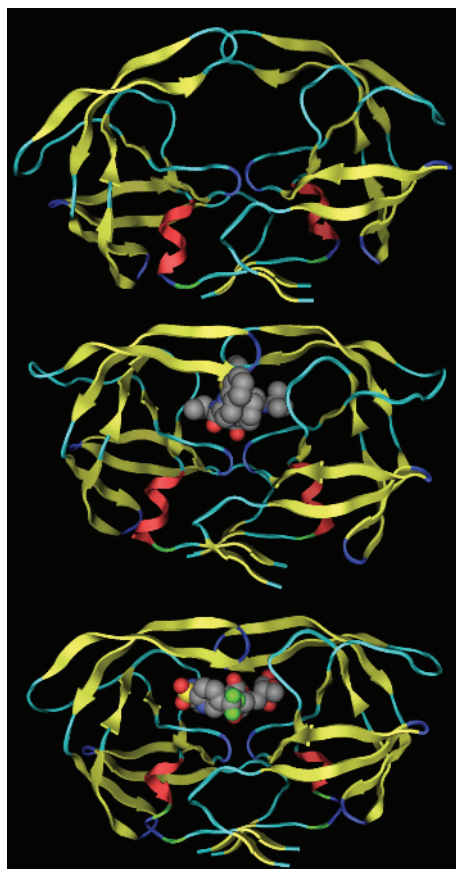


**Figure 1.27** Conserved features of relatively weak lead peptide substrates (colored red), with truncations and alterations (colored black) and the addition of new features (colored blue) for Palinavir and Tipranavir, together with bound crystal structures of each.

**Table 1.8** Inhibition of HIV-1 and HIV-2 proteases by Palinavir and activity against human aspartyl proteases

Aspartyl Protease	EC <sub>50</sub> (nM)
HIV-1	4 (0.031 <sup>a</sup> )
HIV-2	10 (0.134 <sup>a</sup> )
Renin	> 50 000
Cathepsin D	100 000
Pepsin	33 000
Gastricsin	45 000

<sup>a</sup>K<sub>i</sub> was determined by a steady-state velocity method.

was stopped just before entering clinical trials. In a separate program, a non-peptidic drug was rationally discovered and is now marketed as Tipranavir (Figure 1.27). Tipranavir possesses a complimentary resistance profile to that seen with other peptidomimetic drugs in this class [99–101].

## 1.8 Conclusions

Historically, the process of taking a peptide hit and turning this into a marketed, orally bioavailable drug has been time consuming and prone to failure. Through the process outlined in this chapter (Schemes 1.1 and 1.2), resting on a “sense-making” approach to the creation of knowledge and understanding of the therapeutic target of interest and how the peptide starting point(s) interact with this target, the success rate in taking a peptide and creating an orally bioavailable peptide mimic can be increased. We have exemplified this process in detail for two targets: HCMV protease and HCV protease and have teased out important strategic peptide mimic design considerations for a number of other targets such as herpes simplex virus, renin aspartyl protease, and HIV protease. As a testament to the approach taken to peptide mimic design outlined here, we have delivered a number of clinical candidates, including the HCV protease inhibitors BILN 2061 and BI00201335, which are currently in Phase III clinical trials.

Although a number of important design stage posts will be present in any peptide to peptide mimic program, important points for consideration include mapping of the critical binding elements of the substrate to the protein (determining the bioactive conformation of the inhibitor), increasing peptide potency where necessary in order to generate meaningful SAR, often by incorporating a warhead; remembering to remove the warhead in later medicinal chemistry design iterations when appropriate. Additionally, through truncation of the peptide, to find the minimally active peptide and building back potency (and concurrently de-peptidizing), in part through matching of the inhibitor’s free-state conformation to its biologically active bound conformation, resulting in a reduction in the entropic cost of binding.

Systematically monitoring the structure and dynamic features of ligands using multidisciplinary strategies has broad application: most bi-molecular interactions involve a range of adaptive processes. Critical to biomolecular recognition events are the necessary structural and flexibility adaptations of the ligand and receptor to attain the bioactive complex. Therefore, peptide to peptide mimic strategies need to recognize these facts and the tactics used need to move to a more holistic approach that incorporates the effects of dynamics and conformational changes, thus moving beyond the simplistic “lock-and-key” and “induced-fit” views of ligand binding to one where we have a better understanding of intermediate events and properties. We believe that by following this strategy and tactics in their application to rational drug design, the discovery process could be accelerated from the knowledge of these

adaptive processes. However, to date, few reports of the application of dynamics and conformational changes have appeared in the literature. The work described here can serve as examples to monitor and exploit adaptive features and will, hopefully, prompt other researchers to incorporate these design strategies into their work.

## References

- 1 Wu, Y.-D. and Gellman, S. (2008) Peptidomimetics. *Acc. Chem. Res.*, **41**, 1231–1232.
- 2 Gante, J. (1994) Peptide mimics – tailor-made enzyme inhibitors. *Angew. Chem., Int. Ed. Engl.*, **33**, 1699–1720.
- 3 Ladner, R.C., Sato, A.K., Gorzelany, J., and de Souza, M. (2004) Phage display-derived peptides as therapeutic alternatives to antibodies. *Drug Discov. Today*, **9**, 525–529.
- 4 Buckingham, S., Quintas, P., and Hopkins, M. (2002) The cost of knowledge, in *B823 Managing Knowledge* (ed. The Open University), Dorset, Henry Ling Ltd., **3**, p. 10.
- 5 LaPlante, S.R. (2007) Exploiting ligand and receptor adaptability in rational drug design using dynamics and structure-based strategies. *Top. Curr. Chem.*, **272**, 259–296.
- 6 Mocarski, E.S. Jr (1995) Cytomegaloviruses and their replication, in *Fields Virology*, **2** (eds B.N. Fields, D.M., Knipe, and P.M. Howley), Lippincott-Raven, Philadelphia, PA, pp. 2447–2492.
- 7 Britt, W.J. and Alford, C.A. (1995) Cytomegalovirus, in *Fields Virology*, **2** (ed. B.N. Fields), Lippincott-Raven, Philadelphia, PA, pp. 2493–2525.
- 8 Casjens, S. and King, J. (1975) Virus assembly. *Annu. Rev. Biochem.*, **44**, 555–611.
- 9 Gibson, W., Welch, A.R., and Hall, M. R.T. (1995) Assembling a herpes virus serine maturational proteinase and new molecular target for antivirals. *Perspect. Drug Discov. Des.*, **2**, 413–426.
- 10 Gao, M., Matusick-Kumar, L., Hurlburt, W., DiTusa, S.F., Newcomb, W.W., Brown, J.C., McCann, P.J. III, Deckman, I., and Colonno, R.J. (1994) The protease of herpes simplex virus type 1 is essential for functional capsid formation and viral growth. *J. Virol.*, **68**, 3702–3712.
- 11 Preston, V.G., Coates, J.A.V., and Rixon, F.J. (1983) Identification and characterization of a herpes simplex virus gene product required for encapsidation of virus DNA. *J. Virol.*, **45**, 1056–1064.
- 12 Matusick-Kumar, L., McCann, P.J. III, Robertson, B.J., Newcomb, W.W., Brown, J.C., and Gao, M. (1995) Release of the catalytic domain N(o) from the herpes simplex virus type 1 protease is required for viral growth. *J. Virol.*, **69**, 7113–7121.
- 13 Tong, L., Qian, C., Massariol, M.-J., Bonneau, P.R., Cordingley, M.G., and Lagacé, L. (1996) A new serine-protease fold revealed by the crystal structure of human cytomegalovirus protease. *Nature*, **383**, 272–275.
- 14 Qiu, X., Culp, J.S., DiLella, A.G., Hellmig, B., Hoog, S.S., Janson, C.A., Smith, W.W., and Abdel-Meguid, S.S. (1996) Unique fold and active site in cytomegalovirus protease. *Nature*, **383**, 275–279.
- 15 Shieh, H.-S., Kurumbail, R.G., Stevens, A.M., Stegeman, R.A., Sturman, E.J., Pak, J.Y., Wittwer, A.J., Palmier, M.O., Wiegand, R.C., Holwerda, B.C., and Stallings, W.C. (1996) Three-dimensional structure of human cytomegalovirus protease. *Nature*, **383**, 279–282.
- 16 Chen, P., Tsuge, H., Almasy, R.J., Gribskov, C.L., Katoh, S., Vanderpool, D.L., Margosiak, S.A., Pinko, C., Matthews, D.A., and Kan, C.-C. (1996)

- Structure of the human cytomegalovirus protease catalytic domain reveals a novel serine protease fold and catalytic triad. *Cell*, **86**, 835–843.
- 17 Margosiak, S.A., Vanderpool, D.L., Sisson, W., Pinko, C., and Kan, C.-C. (1996) Dimerization of the human cytomegalovirus protease: kinetic and biochemical characterization of the catalytic homodimer. *Biochemistry*, **35**, 5300–5307.
  - 18 Darke, P.L., Cole, J.L., Waxman, L., Hall, D.L., Sardana, M.K., and Kuo, L.C. (1996) Active human cytomegalovirus protease is a dimer. *J. Biol. Chem.*, **271**, 7445–7449.
  - 19 Bonneau, P.R., Grand-Maitre, C., Greenwood, D.J., Lagacé, L., LaPlante, S.R., Massariol, M.-J., Ogilvie, W.W., O'Meara, J.A., and Kawai, S.H. (1997) Evidence of a conformational change in the human cytomegalovirus protease upon binding of peptidyl-activated carbonyl inhibitors. *Biochemistry*, **36**, 12644–12652.
  - 20 LaPlante, S.R., Bonneau, P.R., Aubry, N., Cameron, D.R., Déziel, R., Grand-Maitre, C., Plouffe, C., Tong, L., and Kawai, S.H. (1999) Characterization of the human cytomegalovirus protease as an induced-fit serine protease and the implications to the design of mechanism-based inhibitors. *J. Am. Chem. Soc.*, **121**, 2974–2986.
  - 21 LaPlante, S.R., Aubry, N., Bonneau, P.R., Cameron, D.R., Lagacé, L., Massariol, M.-J., Montpetit, H., Plouffe, C., Kawai, S.H., Fulton, B.D., Chen, Z.G., and Ni, F. (1998) Human cytomegalovirus protease complexes its substrate recognition sequences in an extended peptide conformation. *Biochemistry*, **37**, 9793–9801.
  - 22 Berger, A. and Schechter, J. (1970) Mapping the active site of papain with the aid of peptide substrates and inhibitors. *Philos. Trans. R. Soc. London, Ser. B.*, **257**, 249–264.
  - 23 Sardana, V.V., Wolfgang, J.A., Veloski, C.A., Long, W.J., Legrow, K., Wolanski, B., Emimi, E.A., and LaFemina, R.L. (1994) Peptide substrate cleavage specificity of the human cytomegalovirus protease. *J. Biol. Chem.*, **269**, 14337–14340.
  - 24 Ni, F. (1994) Recent developments in transferred NOE methods. *Prog. NMR Spectrosc.*, **26**, 517–606.
  - 25 LaFemina, R.L., Bakshi, K., Long, W.J., Pramanik, B., Veloski, C.A., Wolanski, B.S., Marcy, A.I., and Hazuda, D.J. (1996) Characterization of a soluble stable human cytomegalovirus protease and inhibition by M-site peptide mimics. *J. Virol.*, **70**, 4819–4824.
  - 26 Fersht, A. (ed.) (1985) *Enzyme Structure and Mechanisms*, 2nd edn, Freeman and Co, New York.
  - 27 Polgár, L. (ed.) (1989) *Mechanisms of Protease Action*, CRC Press Inc, Boca Raton FL, Chapter 3.
  - 28 Hedstrom, L. (2002) Serine protease mechanism and specificity. *Chem. Rev.*, **102**, 4501–4524.
  - 29 Mercer, D.F., Schiller, D.E., Elliott, J.F., Douglas, D.N., Hao, C., Rinfret, A., Addison, W.R., Fischer, K.P., Churchill, T.A., Lakey, J.R.T., Tyrrell, D.L.J., and Kneteman, N.M. (2001) Hepatitis C virus replication in mice with chimeric human livers. *Nature Medicine*, **7**, 927–933.
  - 30 Ogilvie, W.W., Bailey, M., Poupart, M.-A., Abraham, A., Bhavsar, A., Bonneau, P.R., Bordeleau, J., Bousquet, Y., Chabot, C., Duceppe, J.-S., Fazal, G., Goulet, S., Grand-Maitre, C., Guse, I., Halmos, T., Lavallée, P., Leach, M., Malenfant, E., O'Meara, J.A., Plante, R., Plouffe, C., Poirier, M., Soucy, F., Yoakim, C., and Déziel, R. (1997) Peptidomimetic inhibitors of the human cytomegalovirus protease. *J. Med. Chem.*, **40**, 4113–4135.
  - 31 LaPlante, S.R., Cameron, D.R., Aubry, N., Bonneau, P.R., Déziel, R., Grand-Maitre, C., Ogilvie, W.W., and Kawai, S.H. (1998) The conformation of a peptidyl methyl ketone inhibitor bound to the human cytomegalovirus protease. *Angew. Chem. Int. Ed. Engl.*, **37**, 2729–2732.
  - 32 Tong, L., Qian, C., Massariol, M.-J., Déziel, R., Yoakim, C., and Lagacé, L. (1998) Conserved mode of

- peptidomimetic inhibition and substrate recognition of human cytomegalovirus protease. *Nature Struct. Biol.*, **5**, 819–826.
- 33 Cao, Y., Musah, R.A., Wilcox, S.K., Goodin, D.B., and Mcrec, D.E. (1998) Protein conformer selection by ligand binding observed with crystallography. *Protein Sci.*, **7**, 72–78.
- 34 LaPlante, S.R., Llinàs-Brunet, M. (2005) Dynamics and structure-based design of drugs targeting the critical serine protease of the Hepatitis C Virus – from a peptide substrate to BILN 2061. *Curr. Med. Chem.*, **4**, 111–132.
- 35 Choo, Q.L., Kuo, G., Weiner, A.J., Overby, L.R., Bradley, D.W., and Houghton, M. (1989) Isolation of a cDNA clone derived from a blood-borne non-A, non-B viral hepatitis genome. *Science*, **244**, 359–362.
- 36 Kuo, G., Choo, Q.L., Alter, H.J., Gitnick, G.L., Redeker, A.G., Purcell, R.H., Miyamura, T., Dienstag, J.L., Alter, M.J., and Stevens, C.E. (1989) An assay for circulating antibodies to a major etiologic virus of human non-A, non-B hepatitis. *Science*, **244**, 362–364.
- 37 Di Bisceglie, A.M. (1998) Hepatitis C. *Lancet*, **351**, 351–355.
- 38 World Health Organization (1999) Global surveillance and control of hepatitis C. Report of a WHO consultation organized in collaboration with the viral hepatitis prevention board, Antwerp, Belgium. *J. Virol. Hepat.*, **6**, 35–47.
- 39 Kakiuchi, N., Hijikata, M., Komoda, Y., Tanji, Y., Hirowatari, Y., and Shimotohno, K. (1995) Bacterial expression and analysis of cleavage activity of HCV serine proteinase using recombinant and synthetic substrate. *Biochem. Biophys. Res. Comm.*, **210**, 1059–1065.
- 40 Llinàs-Brunet, M., Bailey, M., Fazal, G., Goulet, S., Halmos, T., LaPlante, S., Maurice, R., Poirier, M., Poupart, M.-A., Thibeault, D., Wernic, D., and Lamarre, D. (1998) Peptide-based inhibitors of the hepatitis C virus serine protease. *Bioorg. Med. Chem. Lett.*, **8**, 1713–1718.
- 41 Llinàs-Brunet, M., Bailey, M., Déziel, R., Fazal, G., Gorys, V., Goulet, S., Halmos, T., Maurice, R., Poirier, M., Poupart, M.-A., Rancourt, J., Thibeault, D., Wernic, D., and Lamarre, D. (1998) Studies on the C-terminal of hexapeptide inhibitors of the hepatitis C virus serine protease. *Bioorg. Med. Chem. Lett.*, **8**, 2719–2724.
- 42 Bailey, M., Halmos, T., Goudreau, N., Lescop, E., and Llinàs-Brunet, M. (2004) Novel azapeptide inhibitors of hepatitis C virus serine protease. *J. Med. Chem.*, **47**, 3788–3799.
- 43 LaPlante, S.R., Cameron, D.R., Aubry, N., Lefebvre, S., Kukolj, G., Maurice, R., Thibeault, D., Lamarre, D., and Llinàs-Brunet, M. (1999) Solution structure of substrate – based ligands when bound to hepatitis C virus NS3 protease domain. *J. Biol. Chem.*, **274**, 18618–18624.
- 44 Llinàs-Brunet, M., Bailey, M., Fazal, G., Ghire, E., Gorys, V., Goulet, S., Halmos, T., Maurice, R., Poirier, M., Poupart, M.-A., Rancourt, J., Thibeault, D., Wernic, D., and Lamarre, D. (2000) Highly potent and selective peptide-based inhibitors of the hepatitis C virus serine protease: towards smaller inhibitors. *Bioorg. Med. Chem. Lett.*, **10**, 2267–2270.
- 45 LaPlante, S.R., Aubry, N., Bonneau, P., Kukolj, G., Lamarre, D., Lefebvre, S., Li, H., Llinàs-Brunet, M., Plouffe, C., and Cameron, D.R. (2000) NMR line-broadening and transferred NOESY as a medicinal chemistry tool for studying inhibitors of the hepatitis c virus NS3 protease domain. *Bioorg. Med. Chem. Lett.*, **10**, 2271–2274.
- 46 Rancourt J., Cameron, D.R., Gorys, V., Lamarre, D., Poirier, M., Thibeault, D., and Llinàs-Brunet, M. (2004) Peptide-based inhibitors of the hepatitis C virus NS3 protease: structure-activity relationship at the C-terminal position. *J. Med. Chem.*, **47**, 2511–2522.
- 47 Pause, A., Kukolj, G., Bailey, M., Brault, M., Do, F., Halmos, T., Lagace, L., Maurice, R., Marquis, M., McKercher, G., Pellerin, C., Pilote, L., Thibeault, D., and Lamarre, D. (2003)

- An NS3 serine protease inhibitor abrogates replication of subgenomic hepatitis C virus RNA. *J. Biol. Chem.*, **278**, 20374–20380.
- 48 Poupert, M.-A., Cameron, D.R., Chabot, C., Ghiron, E., Goudreau, N., Goulet, S., Poirier, M., and Tsantrizos, Y. (2001) Solid-phase synthesis of peptidomimetic inhibitors for the hepatitis C virus NS3 protease. *J. Org. Chem.*, **66**, 4743–4751.
- 49 Goudreau, N., Cameron, D.R., Bonneau, P., Gorys, V., Plouffe, C., Poirier, M., Lamarre, D., and Llinàs-Brunet, M. (2004) NMR structural characterization of peptide inhibitors bound to the hepatitis C virus NS3 protease: design of a new P2 substituent. *J. Med. Chem.*, **47**, 123–132.
- 50 Tsantrizos, Y., Bolger, G., Bonneau, P., Cameron, D.R., Goudreau, N., Kukolj, G., LaPlante, S.R., Llinàs-Brunet, M., Nar, H., and Lamarre, D. (2003) Macrocytic inhibitors of the NS3 protease as potential therapeutic agents of hepatitis C virus infection. *Angew. Chem. Int. Ed. Engl.*, **42**, 1356–1360.
- 51 LaPlante, S.R., Aubry, N., Déziel, R., Ni, F., and Xu, P. (2000) Transferred 13C T1 relaxation at natural isotopic abundance: a practical method for determining site-specific changes in ligand flexibility upon binding to a macromolecule. *J. Am. Chem. Soc.*, **122e**, 12530–12532.
- 52 Llinàs-Brunet, M., Bailey, M.D., Ghiron, E., Gorys, V., Halmos, T., Poirier, M., Rancourt, J., and Goudreau, N. (2004) A systematic approach to the optimization of substrate-based inhibitors of the hepatitis C virus NS3 protease: discovery of potent and specific tripeptide inhibitors. *J. Med. Chem.*, **47**, 6584–6594.
- 53 Goudreau, N., Brochu, C., Cameron, D.R., Duceppe, J.-S., Faucher, A.-M., Ferland, J.-M., Grand-Maitre, C., Poirier, M., Simoneau, B., and Tsantrizos, Y.S. (2004) Potent inhibitors of the hepatitis C virus NS3 protease: design and synthesis of macrocyclic substrate-based -strand mimics. *J. Org. Chem.*, **69**, 6185–6201.
- 54 Ali, S., Pellerin, C., Lamarre, D., and Kukolj, G. (2004) Hepatitis C virus subgenomic replicons in the human embryonic kidney 293 cell line. *J. Virol.*, **78**, 491–501.
- 55 Llinàs-Brunet, M., Bailey, M., Bolger, G., Brochu, C., Faucher, A.M., Ferland, J.-M., Garneau, M., Ghiron, E., Gorys, V., Grand-Maitre, C., Halmos, T., Lapayre-Pachette, N., Liard, F., Poirier, M., Rheame, M., Tsantrizos, Y.S., and Lamarre, D. (2004) Structure-activity study on a novel series of macrocyclic inhibitors of the hepatitis C virus NS3 protease leading to the discovery of BILN 2061. *J. Med. Chem.*, **47**, 1605–1608.
- 56 Thibeault, D., Bousquet, C., Gingras, R., Lagace, L., Maurice, R., White, P., and Lamarre, D. (2004) Sensitivity of NS3 serine proteases from hepatitis C virus genotypes 2 and 3 to the inhibitor BILN 2061. *J. Virol.*, **78**, 7352–7359.
- 57 Faucher, A.-M., Bailey, M., Beaulieu, P. L., Brochu, C., Duceppe, J.-S., Ferland, J.-M., Ghiron, E., Gorys, V., Halmos, T., Kawai, S.H., Poirier, M., Simoneau, B., Tsantrizos, Y.S., and Llinàs-Brunet, M. (2004) Synthesis of BILN 2061, an HCV NS3 protease inhibitor with proven antiviral effect in humans. *Org. Lett.*, **6**, 2901–2904.
- 58 Lamarre, D., Anderson, P.C., Bailey, M., Beaulieu, P., Bolger, G., Bonneau, P., Bös, M., Cameron, D.R., Cartier, M., Cordingley, M.G., Faucher, A.-M., Goudreau, N., Kawai, S.H., Kukolj, G., Lagace, L., LaPlante, S.R., Narjes, H., Poupert, M.-A., Rancourt, J., Sentjens, R.E., St George, R., Simoneau, B., Steinmann, G., Thibeault, D., Tsantrizos, Y.S., Weldon, S.M., Yong, C.L., and Llinàs-Brunet, M. (2003) An NS3 protease inhibitor with antiviral effects in humans infected with hepatitis C virus. *Nature*, **426**, 186–189.
- 59 Hinrichsen, H., Benhamou, Y., Wedemeyer, H., Reiser, M., Sentjens, R.E., Calleja, J.L., Forn, X., Erhardt, A., Cronlein, J., Chaves, R.L., Yong, C.L., Nehmiz, G., and Steinmann, G.G.

- (2004) Short-term antiviral efficacy of BILN 2061, a hepatitis C virus serine protease inhibitor, in hepatitis C genotype 1 patients. *Gastroenterology*, **127**, 1347–1355.
- 60 Venkatraman, S. and Njoroge, F.G. (2009) Macrocyclic inhibitors of HCV NS3 protease. *Expert Opinion on Therapeutic Patents*, **19**, 1277–1303.
- 61 Llinàs-Brunet, M., Bailey, M.D., Goudreau, N., Bhardwaj, P.K., Bordeleau, J., Bös, M., Bousquet, Y., Cordingley, M.G., Duan, J., Forgione, P., Garneau, M., Ghiro, E., Gorys, V., Goulet, S., Halmos, T., Kawai, S.H., Naud, J., Poupart, M.-A., and White, P.W. (2010) The discovery of BI 201335: a potent and selective non-covalent inhibitor of the hepatitis C Virus NS3 protease. *J. Med. Chem.*, **53**, 6466–6476
- 62 Manns, M.P., Bourlière, M., Benhamou, Y., Pol, S., Bonacini, M., Trepo, C., Wright, D., Berg, T., Calleja, J.L., White, P.W., Stern, J.O., Steinmann, G., Yong, C.L., Kukolj, G., Scherer, J., and Boecher, W.O. (2010) Potency, safety and pharmacokinetics of the NS3/4A protease inhibitor BI201335 in patients with chronic HCV genotype-1 infection. *J. Hepatol.*, **54**, 1114–1122.
- 63 Lammers, M. and Follman, H. (1983) The ribonucleotide reductases – a unique group of metalloenzymes essential for cell proliferation. *Struct. Bonding*, **54**, 27–91.
- 64 Ingemarson, R. and Lankinen, H. (1987) The herpes simplex virus type 1 ribonucleotide reductase is a tight complex of the type  $\alpha 2\beta 2$  composed of 40K and 140K proteins, of which the latter shows multiple forms due to proteolysis. *Virology*, **156**, 417–422.
- 65 Filatov, D., Ingemarson, R., Graslund, A., and Thelander, L. (1992) The role of herpes simplex virus ribonucleotide reductase small subunit carboxyl terminus in subunit interaction and formation of iron-tyrosyl center structure. *J. Biol. Chem.*, **267**, 15816–15822.
- 66 Krogsrud, R.L., Welchner, E., Scouten, E., and Liuzzi, M. (1993) A solid-phase assay for the binding of peptidic subunit association inhibitors to the herpes simplex virus ribonucleotide reductase large subunit. *Anal. Biochem.*, **213**, 386–394.
- 67 Chang, L.L., Hannah, J., Ashton, W.T., Rasmusson, G.H., Ikeler, T.J., Patel, G.F., Garsky, V., Uncapher, C., Yamanaka, G., McClements, W.L., and Tolman, R.L. (1992) Substituted penta- and hexapeptides as potent inhibitors of herpes simplex virus type 2 ribonucleotide reductase. *Bioorg. Med. Chem. Lett.*, **2**, 1207–1212.
- 68 Gaudreau, P., Brazeau, P., Richer, M., Cormier, J., Langlois, D., and Langelier, Y. (1992) Structure–function studies of peptides inhibiting the ribonucleotide reductase activity of herpes simplex virus type I. *J. Med. Chem.*, **35**, 346–350.
- 69 Liuzzi, M. and Déziel, R. (1993) *The Search for Antiviral Drugs* (eds J. Adams and V.J. Merluzzi), Birkhauser, Boston, pp. 225–238.
- 70 Moss, N., Déziel, R., Adams, J., Aubry, N., Bailey, M., Baillet, M., Beaulieu, P., DiMaio, J., Duceppe, J.-S., Ferland, J.-M., Gauthier, J., Ghiro, E., Goulet, S., Grenier, L., Lavallée, P., Lépine-Frenette, C., Plante, R., Rakhit, S., Soucy, F., Wernic, D., and Guindon, Y. (1993) Inhibition of herpes simplex virus type 1 ribonucleotide reductase by substituted tetrapeptide derivatives. *J. Med. Chem.*, **36**, 3005–3009.
- 71 LaPlante, S.R., Aubry, N., Liuzzi, M., Thelander, L., Ingemarson, R., and Moss, N. (1994) The critical C-terminus of the small subunit of herpes simplex virus ribonucleotide reductase is mobile and conformationally similar to C-terminal peptides. *Int. J. Peptide Protein Res.*, **44**, 549–555.
- 72 Nordlund, P., Sjöberg, B.-M., and Eklund, H. (1990) Three-dimensional structure of the free radical protein of ribonucleotide reductase. *Nature (London)*, **345**, 593–598.

- 73 Stubbe, J. (1990) Ribonucleotide reductases: amazing and confusing. *J. Biol. Chem.*, **265**, 5329–5332.
- 74 Moss, N., Déziel, R., Ferland, J.-M., Goulet, S., Jones, P.-J., Leonard, S.F., Pitner, P., and Plante, R. (1994) Herpes Simplex virus ribonucleotide reductase subunit association inhibitors: the effect and conformation of -alkylated aspartic acid derivatives. *Bioorg. Med. Chem.*, **2**, 959–970.
- 75 Brandt, C.R., Spencer, B., Imesch, P., Garneau, M., and Déziel, R. (1996) Evaluation of a peptidomimetic ribonucleotide reductase inhibitor with a murine model of herpes simplex virus type 1 ocular disease. *Antimicrob. Agents Chemother.*, **40**, 1078–1084.
- 76 Llinàs-Brunet, M., Moss, N., Scouten, E., Liuzzi, M., and Déziel, R. (1996) Peptidomimetic inhibitors of herpes virus ribonucleotide reductase, correlation between herpes simplex and varicella zoster virus. *Bioorg. Med. Chem. Lett.*, **6**, 2881–2886.
- 77 Rosenberg, S.H. (1995) Renin inhibitors, in *Progress in Medicinal Chemistry* (eds G.P. Ellis and D.K. Luscombe), Elsevier, New York, pp. 37–114.
- 78 Jung, G.L., Anderson, P.C., Bailey, M., Baillet, M., Bantle, G.W., Berthiaume, S., Lavallée, P., Llinàs-Brunet, M., Thavonekham, B., Thibeault, D., and Simoneau, B. (1998) Novel small renin inhibitors containing 4,5- or 3,5-Dihydroxy-2-substituted-6-phenylhexanamide replacements at the P2–P3 sites. *Bioorg. Med. Chem.*, **6**, 2317–2336.
- 79 Hutchins, C. and Greer, J. (1991) Comparative modeling of proteins in the design of novel renin inhibitors. *Crit. Rev. Biochem. Mol. Biol.*, **26**, 77–127.
- 80 LaPlante, S.R., Tong, L., Aubry, N., Pav, S., Jung, G., and Anderson, P.C. (1996) Several polyhydroxymonamide renin inhibitors assume similar conformations in the unbound and renin-bound states. *Int. J. Peptide Protein Res.*, **48**, 401–410.
- 81 LaPlante, S.R., Tong, L., Aubry, N., Pav, S., Jung, G., and Anderson, P.C. (1995) *Proceedings of the Fourteenth American Peptide Symposium. Peptides: Chemistry, Structure and Biology*, (eds P. T.P. Kaumaya and S.R. Hodges) Mayflower Scientific Ltd., Kingswinford, UK.
- 82 Tong, L., Pav, S., Lamarre, D., Pilote, L., LaPlante, S., Anderson, P., and Jung, G. (1995) High resolution crystal structures of recombinant human renin in complex with polyhydroxymonoamide inhibitors. *J. Mol. Biol.*, **250**, 211–222.
- 83 Simoneau, B., Lavallée, P., Anderson, P. C., Bailey, M., Bantle, G., Berthiaume, S., Chabot, C., Fazal, G., Halmos, T., Ogilvie, W.W., Poupart, M.-A., Thavonekham, B., Xin, Z., Thibeault, D., Bolger, G., Panzenbeck, M., Winquist, R., and Jung, G.L. (1999) Discovery of non-peptidic P2–P3 butanediamide renin inhibitors with high oral efficacy. *Bioorg. Med. Chem.*, **7**, 489–508.
- 84 Luly, J.R., BaMaung, N., Soderquisat, J., Fung, A.K.L., Stein, H., Kleinert, H.D., Marcotte, P.A., Egan, D.A., Bopp, B., Merits, I., Bolis, G., Greer, J., Perun, T.J., and Plattner, J.J. (1988) Renin inhibitors. Dipeptide analogs of angiotensinogen utilizing a dihydroxyethylene transition-state mimic at the scissile bond to impart greater inhibitory potency. *J. Med. Chem.*, **31**, 2264–2276.
- 85 Beaulieu, P.L., Gillard, J., Bailey, M., Beaulieu, C., Duceppe, J.-S., Lavallée, P., and Wernic, D. (1999) Practical synthesis of BILA 2157 BS, a potent and orally active renin inhibitor: use of an enzyme-catalyzed hydrolysis for the preparation of homochiral succinic acid derivatives. *J. Org. Chem.*, **64**, 6622–6634.
- 86 Kohl, N.E., Emini, E.A., Schleif, W.A., Davis, L.J., Heimbach, J.C., Dixon, R.A. F., Scolnick, E.M., and Sigal, I.S. (1988) Active human immunodeficiency virus protease is required for viral infectivity. *Proc. Natl. Acad. Sci. U.S.A.*, **85**, 4686–4690.

- 87 Gottlinger, H.G., Sodroski, J.G., and Haseltine, W.A. (1989) Role of capsid precursor processing and myristoylation in morphogenesis and infectivity of human immunodeficiency virus type 1. *Proc. Natl. Acad. Sci. U.S.A.*, **86**, 5781–5785.
- 88 Peng, C., Ho, B.K., Chang, T.W., and Chang, N.T. (1989) Role of human immunodeficiency virus type 1-specific protease in core protein maturation and viral infectivity. *J. Virol.*, **63**, 2550–2556.
- 89 McQuade, T.J., Tomasselli, A.G., Liu, L., Karacostas, V., Moss, B., Sawyer, T.K., Heinrikson, R.L., and Tarpley, W.G. (1990) A synthetic HIV-1 protease inhibitor with antiviral activity arrests HIV-like particle maturation. *Science*, **247**, 454–456.
- 90 Ratner, L., Haseltine, W., Patarca, R., Livak, K.J., Starcich, B., Josephs, S.F., Doran, E.R., Rafalski, J.A., Whitehorn, E.A., Baumeister, K., Ivanoff, L., Petteway, S.R. Jr, Pearson, M.L., Lautenberger, J.A., Papas, T.S., Ghayeb, J., Chang, N.T., Gallo, R.C., and Wong-Staal, F. (1985) Complete nucleotide sequence of the AIDS virus, HTLV-III. *Nature*, **313**, 277–2.
- 91 Hellen, C.U.T., Krausslich, H.V.G., and Wimmer, E. (1989) Proteolytic processing of polyproteins in the replication of RNA viruses. *Biochemistry*, **28**, 9881–9890.
- 92 Henderson, L.E., Copeland, T.D., Sowder, R.C., Schultz, A.M., and Oroszlan, S. (1988) Analysis of proteins and peptides purified from sucrose gradient banded HTLV-III. UCLA Symposia on Molecular and Cellular Biology, New Series. *Human Retroviruses, Cancer and AIDS: Approaches to Prevention and Therapy*, Liss, New York, pp. 135–147.
- 93 Copeland, T.D., Wondrak, E.M., Tozser, J., Roberts, M.M., and Oroszlan, S. (1990) Substitution of proline with pipercolic acid at the scissile bond converts a peptide substrate of HIV proteinase into a selective inhibitor. *Biochem. Biophys. Res. Commun.*, **169**, 310–314.
- 94 Roberts, N.A., Martin, J.A., Kinchington, D., Broadhurst, A.V., Craig, J.C., Duncan, I.B., Galpin, S.A., Handa, B.K., Kay, J., Krohn, A., Lambert, R.W., Merrett, J.H., Mills, J.S., Parkes, K.E.B., Redshaw, S., Ritchie, A.J., Taylor, D.L., Thomas, G.J., and Machin, P.J. (1990) Rational design of peptide-based HIV proteinase inhibitors. *Science*, **248**, 358–361.
- 95 Tsantrizos, Y.S. (2008) Peptidomimetic therapeutic agents targeting the protease enzyme of the human immunodeficiency virus and hepatitis C virus. *Acc. Chem. Res.*, **41**, 1252–1263.
- 96 Beaulieu, P.L., Wernic, D., Abraham, A., Anderson, P.C., Bogri, T., Bousquet, Y., Croteau, G., Guse, I., Lamarre, D., Liard, F., Paris, W., Thibeault, D., Pav, S., and Tong, L. (1997) Potent HIV protease inhibitors containing a novel (Hydroxyethyl) amide isostere. *J. Med. Chem.*, **40**, 2164–2176.
- 97 Beaulieu, P.L., Lavallée, P., Abraham, A., Anderson, P.C., Boucher, C., Bousquet, Y., Duceppe, J.-S., Gillard, J., Gorys, V., Grand-Maitre, C., Grenier, L., Guindon, Y., Guse, I., Plamondon, L., Soucy, F., Valois, S., Wernic, D., and Yoakim, C. (1997) Practical, stereoselective synthesis of palinavir, a potent HIV protease inhibitor. *J. Org. Chem.*, **62**, 3440–3448.
- 98 Lamarre, D., Croteau, G., Wardrop, E., Bourgon, L., Thibeault, D., Clouette, C., Vaillancourt, M., Cohen, E., Pargellis, C., Yoakim, C., and Anderson, P.C. (1997) Antiviral properties of palinavir, a potent inhibitor of the human immunodeficiency Virus Type 1 protease. *Antimicrob. Agents Chemother.*, **41**, 965–971.
- 99 Baxter, J.D., Schapiro, J.M., Boucher, C.A.B., Kohlbrenner, V.M., Hall, D.B., Scherer, J.R. and Mayers, D.L. (2006) Genotypic changes in human immunodeficiency Virus Type 1 protease associated with reduced susceptibility and virologic response to

- the protease inhibitor tipranavir. *J. Virol.*, **80**, 10794–10801.
- 100** Larder, B.A., Hertogs, K., Bloor, S., van den Eynde, C., DeCianc, W., Wang, Y., Freimuth, W.W., and Tarpley, G. (2000) Tipranavir inhibits broadly protease inhibitor-resistant HIV-1 clinical samples. *AIDS*, **14**, 1943–1948.
- 101** Muzammil, S., Armstrong, A.A., Kang, L.W., Jakalian, A., Bonneau, P.R., Schmelmer, V., Amzel, L.M., and Freire, E. (2007) Unique thermodynamic response of tipranavir to human immunodeficiency Virus Type 1 protease drug resistance mutations. *J. Virol.*, **81**, 5144–5154.

